CORTEX 155 (2022) 107–131

Available online at www.sciencedirect.com

ScienceDirect

Journal homepage: www.elsevier.com/locate/cortex

Research Report

Meta-analytic connectivity modeling of the left and right inferior frontal gyri

Talat Bulut

Department of Speech and Language Therapy, Istanbul Medipol University, Istanbul, Turkey

ARTICLE INFO

Article history:
Received 3 March 2022
Reviewed 24 April 2022
Revised 21 May 2022
Accepted 15 July 2022
Action editor Stephanie Forkel
Published online 3 August 2022

Keywords:
Inferior frontal gyrus
Broca's area
Language
Functional connectivity
Meta-analytic connectivity modeling

ABSTRACT

Background: Neurocognitive models of language processing highlight the role of the left inferior frontal gyrus (IFG) in the functional network underlying language. Furthermore, neuroscience research has shown that IFG is not a uniform region anatomically, cytoarchitectonically or functionally. However, no previous study explored the language-related functional connectivity patterns of IFG subdivisions using a meta-analytic connectivity modeling (MACM) approach.

Purpose: The present MACM study aimed to identify language-related coactivation patterns of the left and right IFG subdivisions.

Method: Six regions of interest (ROIs) were defined using a probabilistic brain atlas corresponding to pars opercularis, pars triangularis and pars orbitalis of IFG in both hemispheres. The ROIs were used to search the BrainMap functional database to identify neuroimaging experiments with healthy, right-handed participants reporting language-related activations in each ROI. Activation likelihood estimation analyses were then performed on the foci extracted from the identified studies to compute functional convergence for each ROI, which was also contrasted with the other ROIs within the same hemisphere.

Results: A primarily left-lateralized functional network was revealed for the left and right IFG subdivisions. The left-hemispheric ROIs exhibited more robust coactivation than the right-hemispheric ROIs. Particularly, the left pars opercularis was associated with the most extensive coactivation pattern involving bilateral frontal, bilateral parietal, left temporal, left subcortical, and right cerebellar regions, while the left pars triangularis and orbitalis revealed a predominantly left-lateralized involvement of frontotemporal regions.

Conclusion: The findings align with the neurocognitive models of language processing that propose a division of labor among the left IFG subdivisions and their respective functional networks. Also, the opercular part of left IFG stands out as a major hub in the language network with connections to diverse cortical, subcortical and cerebellar structures.

E-mail address: tbulut@medipol.edu.tr.
https://doi.org/10.1016/j.cortex.2022.07.003

1. Introduction

It is generally assumed that Broca's area consists of pars opercularis (BA44) and pars triangularis (BA45) of the left inferior frontal gyrus (LIFG) (Amunts et al., 1999; Tremblay & Dick, 2016). However, due to its involvement in language processing, pars orbitalis (BA47) of LIFG has also been viewed as part of a broadly-defined Broca's complex (Xiang, Fonteijn, Norris, & Hagoort, 2010). Previous neuroimaging studies associated parts of this region with syntactic processing (Dapretto & Bookheimer, 1999; Pallier, Devauchelle, & Dehaene, 2011; Segaert, Menenti, Weber, Petersson, & Hagoort, 2012), semantic processing (Dapretto & Bookheimer, 1999; Zhang et al., 2019; Zhu et al., 2019), phonological processing (Heim, Opitz, Müller, & Friederici, 2003; Matsuo et al., 2010), and morphological processing (Bozic, Fonteneau, Su, & Marslen-Wilson, 2015; Laine, Rinne, Krause, Teräs, & Sipilä, 1999; Sahin, Pinker, & Halgren, 2006), among others. In particular, LIFG has frequently been associated with syntactic processing. In support of this association, previous meta-analyses and systematic reviews of neuroimaging research on syntax revealed functional convergence in LIFG, in addition to several other regions including the posterior temporal lobe (Grodzinsky, Pieperhoff, & Thompson, 2021; Hagoort & Indefrey, 2014; Meyer & Friederici, 2016; Rodd, Vitello, Woollams, & Adank, 2015; Walenski, Europa, Caplan, & Thompson, 2019; Zaccarella, Schell, & Friederici, 2017).

Previous research has shown that LIFG is not a uniform region anatomically, cytoarchitectonically or functionally (Amunts et al., 1999; Clos, Amunts, Laird, Fox, & Eickhoff, 2013; Wojtasik et al., 2020). Along similar lines, several studies found that different LIFG subdivisions responded to different linguistic processes, usually involving posterior-dorsal LIFG (BA44) with syntactic processing and anterior-inferior LIFG (BA45 and/or BA47) with semantic processing (Dapretto & Bookheimer, 1999; Schell, Zaccarella, & Friederici, 2017). Furthermore, posterior-dorsal and anterior-inferior portions of LIFG were shown to be differentially involved in phonological and semantic processing, respectively (Devlin, Matthews, & Rushworth, 2003; Gitelman, Nobre, Sonty, Parrish, & Mesulam, 2005; McDermott, Petersen, Watson, & Ojemann, 2003). Several previous meta-analyses also support functional differentiation within LIFG (Hagoort & Indefrey, 2014; Zaccarella et al., 2017; c.f. Rodd et al., 2015), since convergence for semantically challenging sentences was located more anteriorly (BA45) than that for syntactically challenging sentences (BA44) (Hagoort & Indefrey, 2014), and since foci activated for the comparison of syntactically licit sequences versus word lists converged more strongly in BA44 (Zaccarella et al., 2017). Similarly, an activation likelihood estimation meta-analysis of neuroimaging experiments on inflectional morphology also revealed more robust involvement of LBA44 in morphological processing than other LIFG subdivisions, supporting the correlation between posterior LIFG and grammatical processing (Bulut, 2022).

The functional subdivision of LIFG into ventral-dorsal or anterior-inferior-posterior portions has been taken up by several neurocognitive accounts of language processing, in which LIFG plays a pivotal role. That is, anterior-ventral LIFG (usually BA47, but sometimes BA45, as well) is associated with several functions including semantic processing (Friederici, 2011, 2012; Hagoort, 2013), processing declarative memories involving lexical information (Ullman, 2001, 2004, 2016), while posterior-dorsal LIFG (usually BA44, but sometimes BA45, as well) is claimed to underlie syntactic and grammatical processing (Friederici, 2002, 2011, 2012; Hagoort, 2005, 2013, 2016; Ullman, 2001, 2004, 2016), phonological processing (Hagoort, 2005, 2013, 2016), and speech production (Hickok & Poeppel, 2004, 2007; Poeppel, Emmorey, Hickok, & Pylkkanen, 2012). These models also exhibit a certain degree of similarity in their claims of ventral versus dorsal connectivity patterns for the posterior-dorsal versus anterior-ventral portions of LIFG. Despite these similarities, however, there are substantial differences among the models regarding the regions included in these ventral and dorsal networks across the temporal, parietal and frontal lobes, as well as regarding the involvement of subcortical structures. Also, the language network proposed by these models is strongly left-lateralized, with only limited involvement of the right hemisphere (Hickok & Poeppel, 2004, 2007; Poeppel et al., 2012). Although these models have made divergent claims about distinct connectivity patterns of LIFG subdivisions, these claims have not been systematically addressed using a meta-analytic connectivity approach in the language domain.

While the left hemisphere has generally been considered as the dominant hemisphere in language processing, the linguistic role of the right hemisphere has been controversial. Some of the communicative functions attributed in neuroimaging research to the right hemisphere include figurative and metaphorical language processing (Gainotti, 2016, but cf. Cardillo, McQuire, & Chatterjee, 2018), processing contextual and coherent meaning particularly in discourse (Vigneau et al., 2011; Xu, Kemeny, Park, Frattali, & Braun, 2005; Zempleni et al., 1998) and emotional/affective prosody (George et al., 1996; Patel et al., 2018). In parallel with these associations, lesions in the right hemisphere have been reported to involve deficits in pragmatics; i.e., context-dependent use of language and nonverbal elements in communication (Lundgren & Brownell, 2016; Lundgren, Brownell, Cayer-Meade, Milione, & Kearns, 2011; Parola et al., 2016), and emotional prosody (Dara, Bang, Gottesman, & Hillis, 2014; Ross & Mesulam, 1979; Ross & Monnot, 2008; Stockbridge et al., 2021). Previous research also highlighted certain qualitative differences between the two cerebral hemispheres, given that the left hemisphere was shown to interact more with itself especially for certain cognitive functions including language, while the right hemisphere exhibits more bilateral interactions for visuospatial and attentional processes (Gotts et al., 2013). Neuroimaging and neuromodulation studies also emphasized the role that the right-hemisphere, usually RIFG, plays in typical and non-typical language processing and in recovery from aphasia (Galletta, Rao, & Barrett, 2011; Holland & Crinion, 2012; Hummel & Cohen, 2006; Lefaucheur et al., 2017; Torres, Drebing, & Hamilton, 2013). In support of this view, it was found that lateralization of fMRI brain activation associated with picture naming was modulated following repetitive transcranial magnetic stimulation (rTMS) treatment such that more left-lateralized activation was observed for language tasks after compared to before rTMS

intervention (Martin et al., 2009). In a similar vein, a meta-analysis of task-based fMRI studies in people with aphasia (PWA) and healthy controls found that language tasks activated several right frontal regions more in PWA than controls (Stefaniak, Alyahya, & Lambon Ralph, 2021). Despite these associations between the right hemisphere and language processing, much is still unknown about the contributions of the right hemisphere to language processing and about its functional connectivity during language processing.

Although IFG has been central to debates about the relationship between language and the brain, neuroscience research highlights the importance of a functional network for language. Indeed, modern neuroscience has moved away from attributing certain functions to isolated brain regions towards appreciating functional circuitry across the brain underlying cognitive functions (Viñas-Guasch & Wu, 2017). Accordingly, the function of IFG should also be conceptualized as part of a functional and structural neural network for language (Friederici, 2011). Investigations of structural connectivity (Glasser & Rilling, 2008; Parker et al., 2005; Powell et al., 2006) and resting-state functional connectivity (Tomasi & Volkow, 2012; Xiang et al., 2010) of LIFG provided fairly consistent evidence for a frontotemporal network, which has been claimed to underlie language processing. However, several limitations prevent delineating the specifics of a language network based on these techniques. For instance, the limited resolution of diffusion-weighted tractography (DWT) based on the currently available models may pose challenges to linking white matter fibers to specific gray matter sites (Ford et al., 2013; Xiang et al., 2010). Furthermore, the extent to which functional and structural connections revealed in these studies underlie language is questionable as DWT and resting-state fMRI studies identify task-independent general connectivity patterns that may or may not apply to certain cognitive domains. In particular, the inferior frontal cortex and its connections have been associated not only with language, but also with domain-general functions ranging from attention, action processing, working memory, cognitive control to processing emotions, music, math and numbers (Belyk, Brown, Lim, & Kotz, 2017; Clos et al., 2013; Fedorenko, Duncan, & Kanwisher, 2012; Hung et al., 2015; Klimovich-Gray & Bozic, 2019; Maess, Koelsch, Gunter, & Friederici, 2001; Maruyama, Pallier, Jobert, Sigman, & Dehaene, 2012; Novick, Trueswell, & Thompson-Schill, 2005, 2010; Papitto, Friederici, & Zaccarella, 2020; Sebastian et al., 2016; Sundermann & Pfleiderer, 2012; Thothathiri, Schwartz, & Thompson-Schill, 2010). Therefore, IFG arguably assumes its domain-specific linguistic function as a constituent of a wider domain-specific network (Friederici, 2011). However, limited research investigated language-specific connectivity of LIFG, while research into that of RIFG is even more lacking.

A recent development in neuroimaging research which can potentially overcome the aforementioned limitations of structural and resting-state functional connectivity techniques is meta-analytic connectivity modeling (MACM), which computes functional convergence of studies that report activation in a predetermined region of interest (ROI) in a task-dependent or -independent manner (Robinson, Laird, Glahn, Lovallo, & Fox, 2010). Previous meta-analytic connectivity studies of language focused almost exclusively on left-hemispheric regions (Ardila, Bernal, & Rosselli, 2016; Bernal, Ardila, & Rosselli, 2015). One of these studies used MACM to examine connectivity of LBA44 and revealed mainly left-lateralized coactivation patterns across frontal, inferior and superior parietal, and posterior temporal regions (Bernal et al., 2015). However, to better characterize language-related networks of IFG, coactivation patterns of different IFG subdivisions (opercular, triangular and orbital parts) need to be considered, which has not been addressed using a meta-analytic connectivity approach so far. Moreover, despite research showing involvement of right-hemispheric regions in language in healthy and clinical populations, it is surprising that the contributions of RIFG to language have not been systematically addressed in previous research and neurocognitive models of language processing, and no meta-analysis was conducted on language-related functional connectivity of RIFG.

Against this background, the present MACM study aimed to identify language-related coactivation patterns of the left and right IFG subdivisions in healthy participants. To that end, six regions of interest (ROIs) were defined using a probabilistic brain atlas corresponding to pars opercularis (BA44), pars triangularis (BA45) and pars orbitalis (BA47) of IFG in both hemispheres. The ROIs and several criteria were used to search the BrainMap functional database to identify experiments reporting language-related activations in each ROI. Activation likelihood estimation (ALE) analyses were then performed on the foci extracted from the identified studies to compute functional convergence for each one of the ROIs, which was then contrasted with the other ROIs within the same hemisphere. Exploration of the coactivation patterns of IFG subdivisions across language tasks can shed light on the neural network underlying language and constrain neurocognitive models of language processing. In addition, delineating the functional network of language processing in health may provide a baseline against which to compare the language network in clinical populations and assess neurorehabilitation in disorders of language such as aphasia.

2. Materials and methods

The current study used the MACM method to examine the coactivation patterns of three subdivisions of IFG in each hemisphere. For this purpose, the following steps were carried out: Six ROIs (three in each hemisphere) were defined corresponding to opercular, triangular and orbital aspects of IFG based on a cytoarchitectonic, probabilistic brain atlas. The predefined ROIs and additional search criteria were entered in Sleuth to search the BrainMap database in order to identify experiments reporting language-related activations that include the relevant ROI (as well as activations elsewhere in the brain). The activation foci in the identified experiments, which included activations not only within the ROI but also elsewhere in the brain, were extracted using Sleuth and entered in GingerALE, where ALE analyses were performed to identify coactivation network of each ROI. Afterwards, the coactivation network of each ROI was contrasted with the other ROIs within the same hemisphere.

We report how we determined our sample size, all data exclusions (if any), all inclusion/exclusion criteria, whether inclusion/exclusion criteria were established prior to data analysis, all manipulations, and all measures in the study. The study procedures and analyses were not pre-registered prior to the research being conducted.

2.1. Regions of interest

Six ROIs were defined using the probabilistic Julich-Brain atlas, which is based on the brain's cytoarchitecture (Amunts, Mohlberg, Bludau, & Zilles, 2020). Probabilistically defined ROIs offer several advantages over functionally or geometrically defined ones, as the former enable a more consistent characterization across studies and ensure better localization of the target structures (Robinson et al., 2010). Thus, probabilistic atlases help mitigate variations between individual brains (Amunts et al., 2020). Indeed, Broca's area exhibits great individual variability in macro- and micro-anatomy, which may have blurred functional characterization of this region (Amunts et al., 1999; Fedorenko & Blank, 2020). Furthermore, cytoarchitecture is tightly associated with functions and connectivity patterns of brain regions (Amunts et al., 2020; Goulas, Zilles, & Hilgetag, 2018; Wojtasik et al., 2020). Therefore, a probabilistic atlas was used in the present study, as was done in several previous MACM studies (Erickson, Rauschecker, & Turkeltaub, 2017; Riedel et al., 2015; Robinson et al., 2010, 2012). In the present study, the ROIs comprised three structures within LIFG and RIFG, each (Fig. 1). LBA44 and RBA44 comprised the posterior portion of IFG, i.e., pars opercularis, in the left and the right hemispheres, respectively. LBA45 and RBA45 constituted the anterior portion of IFG, i.e., pars triangularis, in the left and the right hemispheres, respectively. More ventrally, LFo6&7 and RFo6&7 spanned parts of the lateral orbitofrontal cortex primarily including BA47, i.e., pars opercularis (Wojtasik et al., 2020). The ROI maps in the MNI Colin 27 template were downloaded from the European Human Brain Project website (https://ebrains.eu), where cytoarchitectonic brain regions are curated and constantly updated (Amunts et al., 2020). The latest versions of the maps as of the preparation of the present study were used; i.e., v9.2 for the left and right BA44 and BA45, and v3.2 for the left and right Fo6&7. The maps were then overlaid on the MNI template (Colin27_T1_seg_MNI.nii) available on GingerALE's website using the Mango software (http://ric.uthscsa.edu/mango/) (Lancaster et al., 2010). LFo6&7 and RFo6&7 were created by combining the Fo6 and Fo7 maps downloaded from the European Human Brain Project website. The probabilistic maps were then thresholded using different probabilities for each ROI (see the color bars in Fig. 1) such that each region had a probability greater than .48, the maximum probability being 1.0 for each region, with mean probabilities ranging from .64 to .77, and a similar size[1] ranging from 2310 mm^3 to 2409 mm^3. Therefore, a balance was struck between the volumetric sizes of the ROIs and their probability of representing respective brain regions to enable direct comparisons among the ROIs. Similar considerations of ROI size and probability were adopted in previous MACM research (Robinson et al., 2010, 2012), and it was pointed out that ROI size differences may lead to identification of disproportionate numbers of experiments, which may complicate comparisons between ROIs (Erickson et al., 2017). Furthermore, thresholding also ensured that there was no overlap among the ROIs. The ROIs were then created based on the thresholded maps. Finally, the ROIs were visually inspected using the Talairach Daemon in Mango (Lancaster et al., 1997, 2000) and using different brain templates in MRIcron (https://www.nitrc.org/projects/mricron) (Rorden & Brett, 2000) to ensure that the intended brain regions were captured.

2.2. Database search

A search was conducted within the BrainMap functional database on 9-27-2021 using Sleuth Version 3.0.4 (Fox et al., 2005; Fox & Lancaster, 2002; Laird, Lancaster, & Fox, 2005). At the time of the search, the functional database comprised 3406 papers, 16,901 experiments, 76,016 subjects and 131,598 locations. The BrainMap taxonomy allows viewing and automatically searching meta-data of articles submitted to the database (Fox et al., 2005; Lancaster et al., 2012). The database search was intended to identify studies on language recruiting only right-handed subjects to identify language-specific connectivity patterns of the ROIs. Thus, the following search query was used: "locations: left and right IFG ROIs", "experimental context: normal mapping", "behavioral domain: cognition-language", "experimental activation: activations only", "subjects: normals", "handedness: right", "imaging modality: fMRI or PET". Restriction of the search to "normals" ensured that only the experiments conducted with healthy subjects were included. The ROIs defined as explained above were separately included as a search criterion in the database searches. The search intended to yield language-related activations; hence, only the "cognition-language" behavioral domain encompassing all linguistic levels (phonology, orthography, semantics, syntax, speech) was used. However, it should be noted that an experiment can be assigned to more than one behavioral domain or subdomain (e.g., both cognition-language and cognition-memory, or both cognition-language-phonology and cognition-language-semantics) depending on the experimental stimuli and task (for details of the BrainMap taxonomy, please refer to Fox et al., 2005; Lancaster et al., 2012, and for explanations of the behavioral domains/subdomains, please refer to https://brainmap.org/taxonomy/behaviors/). The results identified by the database search are summarized in Table 1 below.

The distribution across behavioral subdomains of language-related experiments identified for each ROI and entered in the MACM analyses is shown in Table 2. Table 2 also reports the distribution of experiments across language subdomains in the entire BrainMap database, which was identified using the same search criteria as those for the ROIs except that the ROIs were removed from the search query to identify all language-related experiments in the database

[1] Please see the color bars in Fig. 1 for the minimum and maximum probabilities. The mean probabilities (SDs in parentheses) and sizes of the ROIs were as follows: LBA44: .77 (.09), 2409 mm^3; LBA45: .64 (.12), 2363 mm^3; LFo6&7: .68 (.12), 2353 mm^3; RBA44: .72 (.11), 2391 mm^3; RBA45: .77 (.09), 2310 mm^3; RFo6&7: .64 (.11), 2372 mm^3.

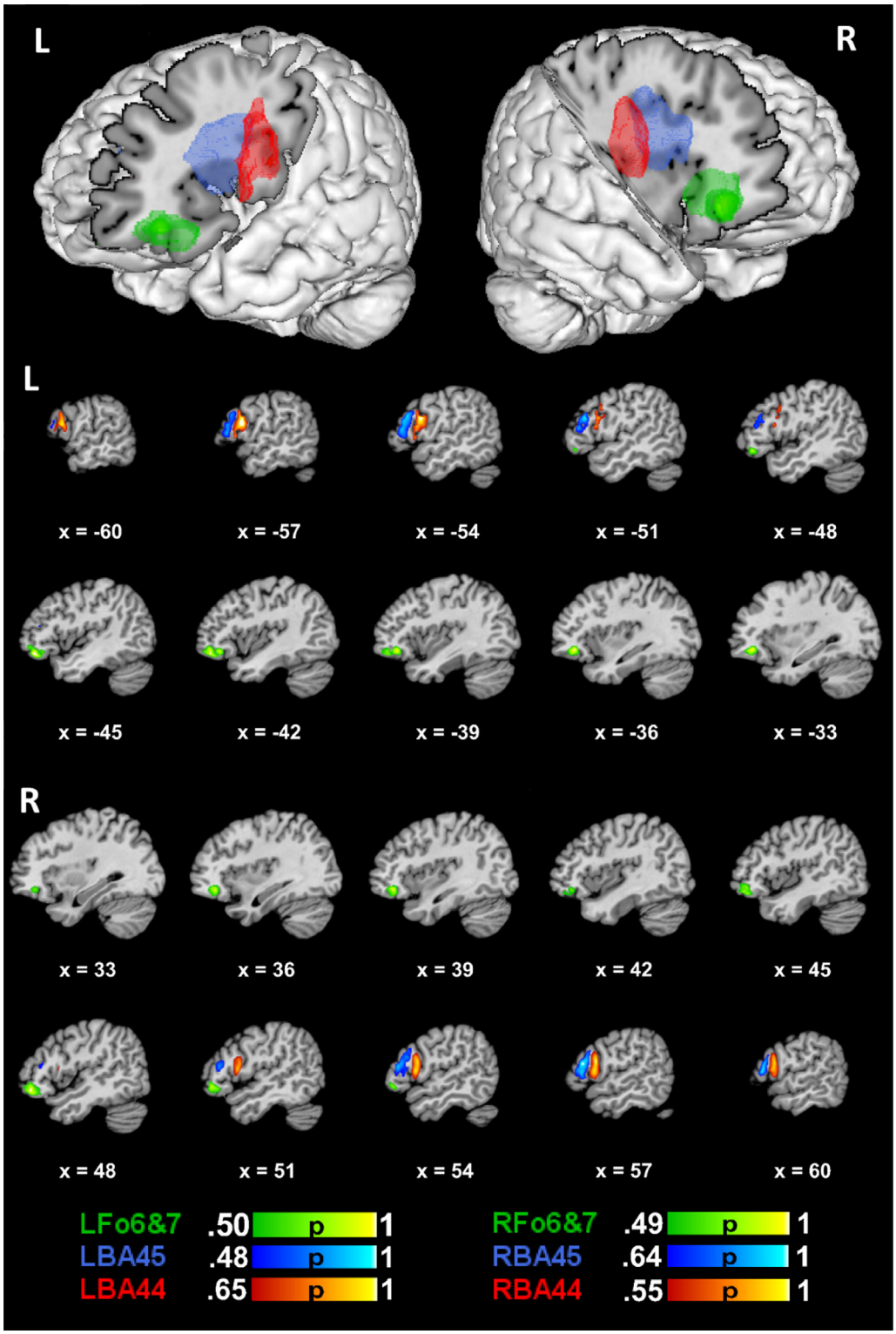

Fig. 1 – Anatomical 3-D renderings of the left and right hemispheric ROIs used in the meta-analysis. BA44 is represented in red, BA45 in blue and Fo6&7 in green for both left and right hemispheres. The color bars indicate probability of the relevant structure to be found in that area. The figure was produced using the Mango software (http://ric.uthscsa.edu/mango/).

reporting coordinates anywhere in the brain. Experiments which were not assigned to a language subdomain, but were solely assigned to the general domain of language are indicated in the 'unspecified' row in Table 2. The Sleuth workspace files with metadata (e.g., citations, experimental information including subject details, stimuli, tasks, behavioral domains/subdomains and contrasts, and technical information including imaging modality) and text files

Table 1 – Database search results for each ROI.

ROI	Papers	Subjects	Experiments	Locations
LBA44	72	1100	95	1394
LBA45	68	926	88	1264
LFo6&7	29	436	34	538
RBA44	22	279	30	492
RBA45	21	298	23	333
RFo6&7	14	240	14	221

containing citations and activation coordinates of the experiments included in each ALE analysis are accessible separately for each ROI in the online repository at https://doi.org/10.17632/nyx2gz9yww.1.

The coordinates identified in each search were grouped by experiment (Turkeltaub, Eickhoff, et al., 2012) and exported as a text file to be input in GingerALE. The icbm2tal transform was used to automatically convert coordinates reported in Talairach space into MNI space (Laird et al., 2010; Lancaster et al., 2007).

2.3. *ALE analyses*

GingerALE 3.0.2 was used (Eickhoff, Bzdok, Laird, Kurth, & Fox, 2012; Eickhoff et al., 2009) to estimate the convergence of coactivations for each ROI. Therefore, six separate ALE analyses were conducted with the activation coordinates obtained for the ROIs. The ALE analyses were performed according to the standard procedures reported in previous research (Cieslik, Mueller, Eickhoff, Langner, & Eickhoff, 2015; Müller et al., 2017; Wojtasik et al., 2020). Thus, 3D Gaussian probability distributions centered at each group of foci were created with a full-width half-maximum (FWHM) that was computed based on the sample size in each experiment (Eickhoff et al., 2009). Next, voxel-wise ALE scores were calculated by obtaining the union of modeled activation maps for each experiment. The union of these activation probabilities were then compared against the null hypothesis of a random spatial relationship between the experiments. The *p*-value distributions resulting from these probabilities were then thresholded at a voxel-level uncorrected cluster-forming threshold of $p < .001$ and a cluster-level corrected threshold of $p < .05$ (family-wise error-corrected for multiple comparisons), with 10,000 thresholding permutations.

Following the coactivation analyses separately for each ROI, the conjunction/intersection of coactivation within each hemisphere was visualized using the "Overlay Logicals" utility of the Mango software (Lancaster et al., 2010). Specifically, the intersection of all ipsilateral ROIs (BA44 ∩ BA45 ∩ Fo6&7 separately in each hemisphere) as well as the intersection of only the opercular and triangular parts of IFG (BA44 ∩ BA45 separately in each hemisphere) were computed. These intersection analyses aimed to identify the coactivation patterns of the Broca's complex in a broad sense including all opercular, triangular and orbital parts (Xiang et al., 2010) as well as that of the more conventionally recognized Broca's area in a narrow sense including only the opercular and triangular parts (Amunts et al., 1999; Tremblay & Dick, 2016), in addition to that of their homologues in the right hemisphere. Finally, contrast/subtraction ALE analyses were performed to compare each ROI with the other two ROIs within the same hemisphere, following the logic of a previous MACM study of three subregions of the superior temporal sulcus (Erickson et al., 2017). Contrast analyses allowed better comparison of the ROIs since they exhibited overlap in coactivation and since one of the aims of the present study was to compare coactivation patterns of different IFG subdivisions. The following contrast analyses were performed: LBA44 > (LBA45 & LFo6&7), LBA45 > (LBA44 & LFo6&7), LFo6&7 > (LBA44 & LBA45); RBA44 > (RBA45 & RFo6&7), RBA45 > (RBA44 & RFo6&7), RFo6&7 > (RBA44 & RBA45). In other words, coactivations of each pair of ROIs in each hemisphere were subtracted from the third ROI within the same hemisphere iteratively using the Contrast Datasets utility in GingerALE, yielding coactivation patterns stronger for each ROI compared to the others. It should be mentioned that the ALE subtraction analysis utilizes permutation significance testing that controls for differences in the number of papers in each comparison set (Eickhoff et al., 2011; Erickson et al., 2017). Given that GingerALE performs contrast analyses based on already thresholded (in the present case, cluster-level FWE corrected) single-dataset images (Eickhoff et al., 2011), and that no cluster-level inference is available in GingerALE for contrast analyses (Hoffman & Morcom, 2018), an uncorrected threshold of $p < .05$ with an extent threshold (minimum cluster size) of 100 mm^3 was applied for the contrast analyses, as implemented in previous studies (D'Astolfo & Rief, 2017; Garrison, Erdeniz, & Done, 2013; Hobeika, Diard-Detoeuf, Garcin, Levy, & Volle, 2016; Kollndorfer et al., 2013; Papitto et al., 2020). The results of the contrast analyses should, therefore, be interpreted with caution.

For both the single ROI coactivation analyses and the contrast analyses, anatomical labels were generated as the nearest gray matter within 5 mm for the activation peaks by the Talairach Daemon embedded in GingerALE (Lancaster et al., 1997, 2000). The results of the performed meta-

Table 2 – Distribution across language subdomains of the experiments entered in the MACM analysis for each ROI and overall distributions across the BrainMap database.

Language subdomain	LBA44	LBA45	LFo6&7	RBA44	RBA45	RFo6&7	BrainMap
Orthography	10	8	4	2	2	2	188
Phonology	25	8	4	7	3	2	295
Semantics	37	59	27	17	15	11	908
Speech	38	30	5	11	7	2	627
Syntax	10	5	2	1	3	1	112
Unspecified	6	6	0	1	1	0	59

analyses were visualized using the Mango software (Lancaster et al., 2010) and overlaid on the MNI template (Colin27_T1_seg_MNI.nii) available on GingerALE's website. The foci extracted from each experiment using Sleuth and entered in the meta-analyses and the GingerALE outputs for each meta-analysis are available in the online repository at https://doi.org/10.17632/nyx2gz9yww.1.

2.4. *Functional decoding*

Functional decoding of the ROIs was performed using the Mango Behavioral Analysis Plugin (Lancaster et al., 2012), which was used in previous research to investigate functional specialization in different brain regions (Erickson et al., 2017; Sundermann & Pfleiderer, 2012). Utilizing the metadata of articles in the BrainMap database, the plugin calculates the observed fraction of activation coordinates for a given behavioral subdomain (e.g., cognition.attention, or cognition.language.phonology) that fall within a prespecified ROI and compares it to the fraction that would be expected if the distribution was random. If the difference between the observed and the expected fraction is high, then the ROI is associated with this behavior. The statistical threshold for significance was determined as a Z-score $\geq$3.0, which corresponds to a one-tailed (testing only positive association) *p*-value of .05 Bonferroni corrected for 51 behavioral subdomains in BrainMap (Lancaster et al., 2012). However, since the purpose of the functional decoding procedure carried out in the present study was to characterize linguistic functions of each ROI, rather than testing their domain-specificity (e.g., language *vs* memory), the analysis was restricted to the phonology, semantics, speech and syntax subdomains. Hence, in the present study, the statistical threshold was set as $Z > 2.24$ (corresponding to a one-tailed *p*-value of .05 Bonferroni corrected for the four subdomains examined). The functional decoding procedure was conducted on the same date as the database search using the same ROIs used for the MACM analysis as described above.

3. Results

Chi-square tests were conducted to examine whether the number of papers and experiments identified for each ROI significantly differed between the left and right hemispheres. It was found that significantly more papers and experiments were identified for each left-hemispheric ROI compared to its right-hemispheric counterpart (BA44: $X^2 > 26.60$, $p < .001$; BA45: $X^2 > 24.82$, $p < .001$; Fo6&7: $X^2 > 5.23$, $p < .022$). This finding shows that more studies in the BrainMap database reported activations in the left IFG than the right IFG for language tasks.

To quantify and compare the extent of coactivation for the ROIs, the coactivation maps for each ROI were analyzed using the Image Statistics utility of Mango, which produced activation details of each slice in the axial, coronal and sagittal planes. Accordingly, each slice with greater than zero active voxels was coded as 1, and each with zero active voxels was coded as 0. These binary data from a total of 493 slices (154, 188 and 151 slices in the axial, coronal and sagittal planes, respectively) were combined and entered in the analyses. A series of chi-square tests were carried out to compare the distributions of active versus non-active slices between the ipsilateral IFG ROIs (Bonferroni-adjusted alpha level for three comparisons in either hemisphere = .017) and between homotopic ROIs across hemispheres. It was found that significantly more extensive coactivation was found for LBA44 (percentage of active slices = 70%) than LBA45 (58%), $X^2 = 15.32$, $p < .001$, and LFo6&7 (45%), $X^2 = 62.79$, $p < .001$, and for LBA45 than LFo6&7, $X^2 = 16.63$, $p < .001$. In RIFG, while RBA44 (52%) and RBA45 (48%) did not exhibit significantly different coactivation distribution, $X^2 = 1.47$, $p = .226$, both of these ROIs coactivated with more extensive regions than RFo6&7 (25%), $X^2 > 57.13$, $p < .001$. When the coactivation distributions of homotopic ROIs across hemispheres were compared, it was found that each LIFG ROI showed more extensive coactivation than its homotopic RIFG counterpart, $X^2 > 10.58$, $p \leq .001$.

3.1. *Coactivations of left-hemispheric ROIs*

The coactivation and intersection results for each LIFG ROIs are visualized in Fig. 2 and the coactivation results are summarized in Table 3. All LIFG ROIs significantly coactivated with ipsilateral regions within the frontal lobe and the temporal lobe (as shown in white in the lower panel of Fig. 2), whereas only LBA44 showed additional coactivation with multiple parietal lobe structures. For all LIFG ROIs, the coactivations within the temporal lobe included BA22, which is commonly considered as Wernicke's area (Tremblay & Dick, 2016). A large overlap of coactivation was observed between LBA44 and LBA45 especially in the frontal lobe ventrally and dorsally, but also in the left insular and temporal cortices. Although LIFG ROIs exhibited a strongly left-lateralized functional network, several right-hemispheric coactivations were also observed, especially for LBA44 (3 clusters and 10 peaks in the right cerebral hemisphere), to a lesser extent for LBA45 (2 clusters, 3 peaks) and none for LFo6&7 (no clusters). The right-hemispheric regions coactivating with both LBA44 and LBA45 include locations in the frontal lobe and the cingulate and insular cortices, while only LBA44 significantly coactivated with the right parietal cortex. Finally, several subcortical coactivations were identified. Only LBA44 showed coactivation in the thalamus, the basal ganglia (putamen) and the claustrum. Although all LIFG ROIs coactivated with parts of the cerebellum, the coactivation peaks for LBA45 and LFo6&7 were parts of a larger cluster together with predominantly fusiform gyrus involvement in the left temporal lobe, while LBA44 coactivated with the right cerebellum (culmen) specifically.

3.2. *Contrasts among left-hemispheric ROIs*

As illustrated in Fig. 3 and detailed in Table 4, the contrast/subtraction results revealed coactivation patterns stronger for each ROI when the coactivation network of each ROI pair was subtracted from the other ROI within the same hemisphere. Each LIFG ROI coactivated with itself, thereby revealing a coactivation pattern in the left IFG reminiscent of the predefined ROI boundary. A more extensive coactivation contrast

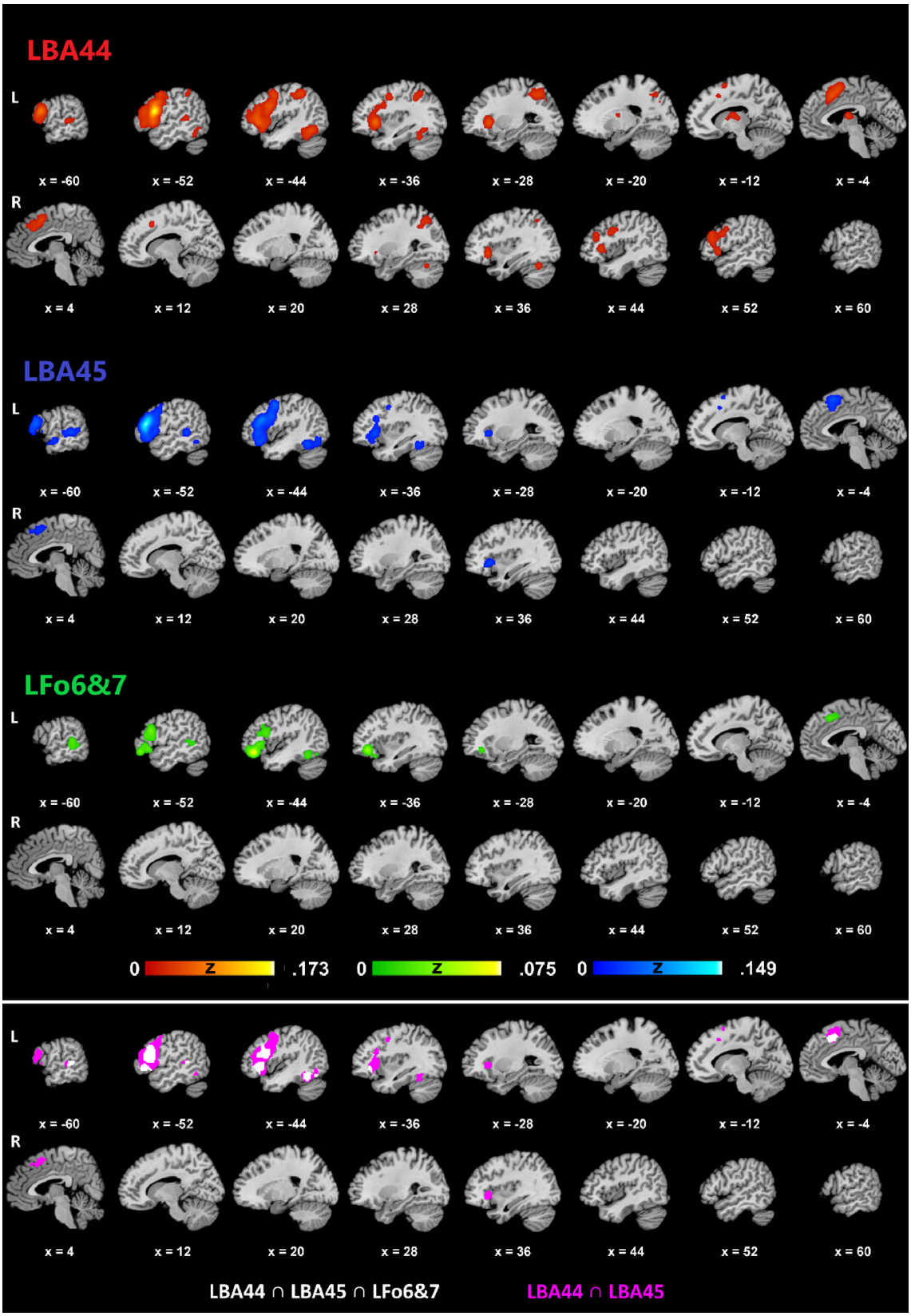

Fig. 2 – Coactivation results for the left-hemispheric ROIs. The upper panel shows the coactivation results for LBA44, LBA45 and LFo6&7 in the left and right hemispheres. The lower panel illustrates the intersection of LBA44, LBA45 and LFo6&7 (white) and of LBA44 and LBA45 (pink).

Table 3 – Coactivation results for the left-hemispheric ROIs.

Anatomical label (Nearest gray matter within 5 mm)	BA	MNI coordinates			ALE	Z	Cluster size (mm^3)
		x	y	z			
LBA44							
L IFG	44	−54	12	18	.173	16.60	41,640
L Claustrum		−32	22	0	.087	9.96	
L IFG	13	−46	28	0	.069	8.36	
L IFG	46	−46	32	10	.061	7.60	
L Precentral Gyrus	6	−46	4	48	.049	6.42	
L MFG	10	−42	46	18	.025	3.62	
L FGmed	32	−4	16	46	.058	7.34	11,144
L FGmed	6	−2	10	50	.055	7.00	
R Cingulate Gyrus	32	8	18	42	.040	5.46	
R Cingulate Gyrus	32	4	24	36	.034	4.83	
R FGmed	8	6	34	40	.029	4.18	
L Cingulate Gyrus	32	−6	24	30	.023	3.35	
R Insula		36	24	−8	.046	6.18	10,672
R MFG	46	50	28	16	.044	5.86	
R IFG	13	42	24	2	.043	5.78	
R MFG	9	50	30	24	.041	5.63	
R IFG	9	48	8	28	.039	5.33	
R Insula	13	50	16	−4	.037	5.19	
L IPL	40	−44	−42	48	.047	6.25	9248
L Precuneus	7	−26	−64	46	.043	5.81	
L SPL	7	−28	−56	46	.043	5.79	
L IPL	40	−38	−46	42	.035	4.91	
L Fusiform Gyrus	37	−44	−58	−14	.051	6.69	6224
L Medial Dorsal Nucleus (Thalamus)		−6	−10	12	.040	5.49	2400
L Putamen (Lentiform Nucleus)		−12	2	6	.023	3.34	
R SPL	7	30	−58	46	.038	5.21	1960
L MTG	22	−60	−32	4	.031	4.43	1816
L STG	22	−54	−40	8	.030	4.34	
R Culmen (Cerebellum)		38	−60	−26	.033	4.70	1352
LBA45							
L IFG	45	−52	28	14	.149	15.29	36,040
L Precentral Gyrus	6	−44	2	46	.057	7.49	
L IFG	9	−44	8	28	.052	6.99	
L IFG	47	−44	26	−14	.049	6.63	
L Insula	13	−34	24	0	.048	6.49	
L IFG	47	−46	22	−10	.047	6.39	
L Precentral Gyrus	44	−54	12	4	.039	5.50	
L SFG	6	−4	16	56	.049	6.60	6792
L FGmed	32	−6	18	44	.037	5.32	
R SFG	8	6	30	48	.024	3.62	
R Cingulate Gyrus	32	6	26	40	.021	3.25	

(continued on next page)

Table 3 – (*continued*)

Anatomical label (Nearest gray matter within 5 mm)	BA	MNI coordinates			ALE	Z	Cluster size (mm^3)
		x	y	z			
L Fusiform Gyrus	37	−44	−52	−18	.046	6.27	5056
L Declive (Cerebellum)		−46	−70	−14	.032	4.74	
L MTG	22	−56	−38	2	.045	6.22	3608
R Insula		38	22	−4	.040	5.63	1840
L MTG	21	−58	−10	−12	.033	4.87	1400
L MTG	21	−58	−2	−18	.028	4.18	
LFo6&7							
L MFG	47	−46	36	−14	.075	10.75	15,440
L IFG	9	−50	18	22	.037	6.64	
L IFG	47	−50	24	−8	.027	5.30	
L IFG	45	−50	26	14	.026	5.14	
L IFG	47	−38	24	−20	.015	3.47	
L MTG	22	−62	−38	4	.027	5.21	3168
L MTG	21	−60	−38	−2	.023	4.72	
L MTG	22	−54	−48	2	.019	4.04	
L Fusiform Gyrus	37	−46	−52	−18	.024	4.77	1480
L Declive (Cerebellum)		−46	−68	−18	.016	3.61	
L FGmed	6	−6	20	44	.024	4.81	1400

Note: MNI coordinates correspond to cluster peaks. L: Left, R: Right, FGmed: Medial frontal gyrus, IFG: Inferior frontal gyrus, IPL: Inferior parietal lobule, ITG: Inferior temporal gyrus, MFG: Middle frontal gyrus, MTG: Middle temporal gyrus, SFG: Superior frontal gyrus, SPL: Superior parietal lobule, STG: Superior temporal gyrus.

network was identified for LBA44 (14 clusters, 29 peaks) than LBA45 (3 clusters, 3 peaks) and LFo6&7 (3 clusters, 8 peaks). In the left hemisphere, LBA44 exhibited a more robust dorsal coactivation pattern extending into the precentral gyrus in the frontal lobe and into the inferior and superior parietal lobule including the precuneus. LBA45 and LFo6&7, on the other hand, revealed a more ventral distribution spanning only the frontal and temporal lobes. Within the temporal lobe, LBA44 showed stronger coactivation solely in the fusiform gyrus, except for a single peak at STG which was a tiny part (1.6%) of a much larger frontal cluster. However, LBA45 and LFo6&7 coactivated more strongly with the anterior and posterior MTG, respectively. Also, only LBA44 revealed stronger coactivation in the left insula, while only LFo6&7 strongly coactivated with the left cingulate gyrus. As for the coactivation patterns in the right hemisphere, only LBA44 showed right-hemispheric coactivation in the frontal lobe (middle and superior frontal gyri, precentral gyrus), parietal lobe (precuneus) and the cingulate gyrus. The extensive coactivation network strongly associated with LBA44 also spanned left-hemispheric subcortical structures (claustrum, thalamus) and the culmen in the right cerebellar hemisphere.

3.3. *Coactivations of right-hemispheric ROIs*

Coactivation results for RIFG ROIs are shown in Fig. 4 and Table 5. Unlike LIFG results, there was almost no overlap among all three ROIs in either the left or the right hemisphere,

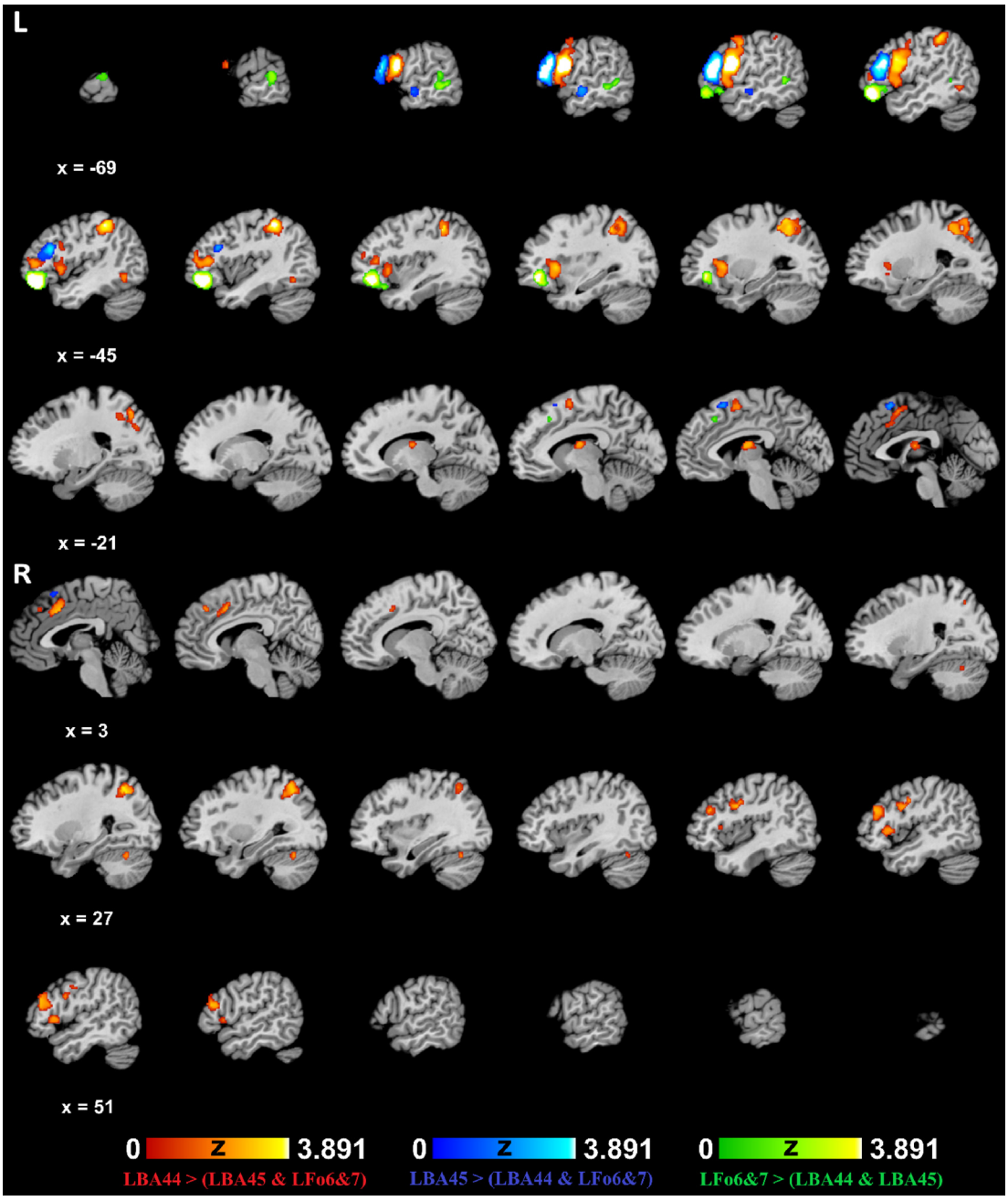

Fig. 3 – Contrast results for the left-hemispheric ROIs.

while RBA44 and RBA45 exhibited coactivation overlap in the left and right frontal and insular cortices. Within the right hemisphere, RIFG ROIs coactivated almost exclusively with frontal regions, except for the right insular coactivation for RBA44 and RBA45, and for the coactivation in the right anterior STG, which was part of a larger frontal cluster, for RBA44. In the contralateral left hemisphere, on the other hand, more widespread coactivation was observed for all RIFG ROIs. RBA44 and RBA45 also coactivated with the parietal lobe (different sites within the inferior parietal lobule). All RIFG ROIs involved homotopic coactivation patterns with the left-hemispheric mirror regions, which extended into surrounding regions within IFG and MFG (for all RIFG ROIs), the precentral gyrus and the medial frontal gyrus (for RBA44 and RBA45) and SFG (for RBA44). All right-hemispheric ROIs also coactivated with the posterior temporal regions, with RBA44 exhibiting coactivation with a more superior site (MTG) than RBA45 and RFo6&7 (fusiform gyrus). In addition, RBA44 was associated with significant coactivation in the left insular and cingulate cortices. Finally, subcortical coactivations were identified for RBA44 (left thalamus) and RBA45 (left and right claustra).

3.4. *Contrasts among right-hemispheric ROIs*

The contrast results for the right-hemispheric ROIs are shown in Fig. 5 and Table 6. Each ROI exhibited strong coactivation with itself. A more extensive coactivation contrast network

Table 4 – Contrast results for the left-hemispheric ROIs.

Anatomical label (Nearest gray matter within 5 mm)	BA	MNI coordinates			Z	Cluster size (mm^3)
		x	y	z		
LBA44 > (LBA45 & LFo6&7)						
L IFG	44	−55.4	8.9	18.7	3.89	9520
L Precentral Gyrus	6	−54	−2	42	2.97	
L Insula	13	−48	10	0	2.53	
L STG	22	−54	12	−2	2.37	
L Precentral Gyrus	6	−54	6	48	2.05	
L IPL	40	−41	−40.5	49	3.89	6288
L SPL	7	−30	−52	54	3.43	
L SPL	7	−29.2	−53.6	46.4	3.01	
L Precuneus	7	−30	−44	48	3.29	
No gray matter found		−28	−52	40	3.16	
L SPL	7	−22	−68	52	2.78	
L Precuneus	7	−20	−68	44	2.30	
L Claustrum		−32	18	2	3.54	2016
R MFG	46	54	34	18	3.43	1864
R MFG	9	48	34	24	2.82	
R Cingulate Gyrus	32	4	14	38	3.19	1784
L FGmed	6	−8	2	56	2.24	
L MFG	46	−40	34	8	2.79	1560
L MFG	10	−40	44	8	2.41	
R Precuneus	7	26	−62	44	3.89	1536
R Precuneus	7	26	−60	48	3.72	
L Thalamus		−1	−10	12	2.78	888
R Precentral Gyrus	6	42	2	28	2.95	824
R Precentral Gyrus	6	44	−4	32	2.78	
R Precentral Gyrus	44	50	20	2	2.56	744
R Culmen (Cerebellum)		30	−64	−26	2.24	432
L Fusiform Gyrus	37	−46	−60	−8	2.08	392
L Precuneus	31	−22	−72	32	2.29	176
R SFG	8	8	38	40	2.12	144
LBA45 > (LBA44 & LFo6&7)						
L IFG	45	−54.2	28.6	14.3	3.89	7232
L MTG	21	−58	−12	−8	2.59	592
L SFG	6	−4	18	58	2.43	464
LFo6&7 > (LBA44 & LBA45)						
L MFG	47	−42.7	39.4	−13.1	3.89	6640
L IFG	47	−36	22	−22	2.73	
L IFG	47	−54	22	−12	2.14	
L MTG	21	−62	−42	−6	2.77	1472
L MTG	22	−68	−34	6	2.72	
L MTG	21	−58	−50	−2	2.37	
L Temporal Lobe (Sub-Gyral)	37	−54	−52	−2	2.21	
L Cingulate Gyrus	32	−8	26	42	2.03	104

Note: MNI coordinates correspond to cluster peaks. L: Left, R: Right, FGmed: Medial frontal gyrus, IFG: Inferior frontal gyrus, IPL: Inferior parietal lobule, ITG: Inferior temporal gyrus, MFG: Middle frontal gyrus, MTG: Middle temporal gyrus, SFG: Superior frontal gyrus, SPL: Superior parietal lobule, STG: Superior temporal gyrus.

was identified for RBA44 (8 clusters, 17 peaks) than RFo6&7 (5 clusters, 9 peaks) and RBA45 (4 clusters, 7 peaks). In the right-hemisphere, coactivation was restricted to the frontal lobe, with each right-hemispheric ROI strongly coactivating with itself, and with a few other frontal sites including the precentral gyrus (for RBA44), medial frontal gyrus (for RBA44) and SFG (for RFo6&7). In the left hemisphere, all right-hemispheric ROIs showed coactivation within the frontal and temporal lobes, while only RBA44 and RBA45 strongly coactivated with the parietal lobe (inferior parietal lobule). In the left frontal lobe, the right-hemispheric ROIs exhibited homotopic coactivation in and around LIFG (for RBA44 and RFo6&7), MFG (for RBA45 and RFo6&7), the precentral gyrus (for RBA44) and the medial frontal gyrus (for RFo6&7). In the left temporal lobe, RBA45 and RFo6&7 strongly coactivated with the fusiform gyrus, whereas RBA44 showed strong coactivation more superiorly within MTG. In addition, only RBA44 exhibited strong coactivation in the left insula. The right-hemispheric ROIs also revealed subcortical coactivation in the left claustrum (for RBA44) and the left cerebellar hemisphere (declive for RBA45 and culmen for RFo6&7), the latter being parts of larger clusters in the left fusiform gyrus.

3.5. *Functional decoding results*

As shown in Fig. 6, LBA44 was significantly associated with phonology ($Z = 3.34$), semantics ($Z = 2.86$) and speech ($Z = 4.00$), while its association with syntax ($Z = 2.15$) was slightly below the statistical threshold ($Z > 2.24$). Also, LBA45 was only significantly related with semantics ($Z = 2.34$). None of the other ROIs had significant associations with the behavioral subdomains examined.

4. Discussion

The current study investigated language-related coactivation patterns of three cytoarchitectonically-defined subdivisions (pars opercularis/BA44, pars triangularis/BA45, and pars orbitalis/BA47/Fo6&7) of the inferior frontal gyrus in the left and right hemispheres. A series of meta-analytic connectivity modeling analyses identified coactivation maps of these ROIs during language tasks and compared IFG subdivisions through subtraction analyses to reveal coactivation patterns stronger for each ROI. The database search identified more studies reporting coactivations in the left-hemispheric ROIs compared to the right-hemispheric ones. Also, a more widespread and robust coactivation pattern was observed in the left hemisphere than the right for both left- and right-hemispheric ROIs, confirming left-hemispheric dominance of IFG coactivation network for language. Another finding was that LBA44 revealed a more widespread coactivation pattern compared to LBA45 and LFo6&7, highlighting this region as a core component of the functional network for language. The findings from the left- and right-hemispheric ROIs and their implications for neurocognitive models of language processing are discussed below.

4.1. *Coactivation patterns of left-hemispheric ROIs*

The left-hemispheric ROIs coactivated more strongly and extensively with regions in the left hemisphere than with the right hemisphere. LBA44 revealed a more widespread, dorsal coactivation pattern spanning the left frontal, temporal and parietal cortices while the coactivation network of LBA45 and LFo6&7 was mostly restricted ventrally to the frontal and temporal regions. Similar findings were reported in a resting-state functional connectivity study comparing similarly

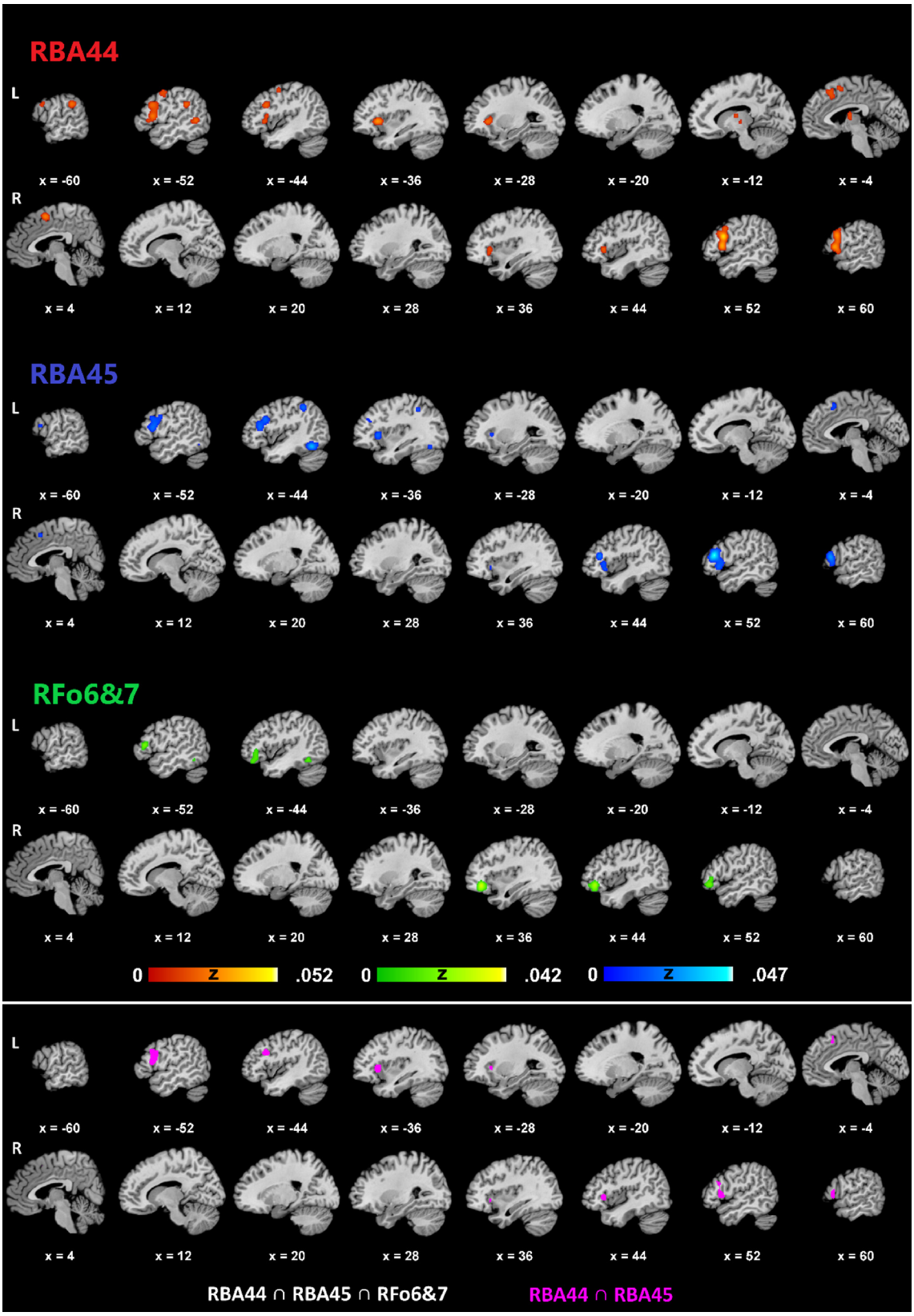

Fig. 4 – Coactivation results for the right-hemispheric ROIs. The upper panel shows the coactivation results for RBA44, RBA45 and RFo6&7 in the left and right hemispheres. The lower panel illustrates the intersection of RBA44, RBA45 and RFo6&7 (white), which revealed only a tiny blob in the left BA45 (at around x = −52, y = 23, z = 11) and the intersection of RBA44 and RBA45 (pink).

Table 5 – Coactivation results for the right-hemispheric ROIs.

Anatomical label (Nearest gray matter within 5 mm)	BA	MNI coordinates			ALE	Z	Cluster size (mm^3)
		x	y	z			
RBA44							
L Insula	13	−36	20	0	.030	6.01	8000
L IFG	44	−50	16	10	.025	5.31	
L IFG	9	−50	16	28	.023	4.97	
R IFG	9	54	14	22	.052	8.81	7400
R Precentral Gyrus	44	56	16	6	.040	7.29	
R MFG	9	56	10	34	.022	4.81	
R STG	22	54	8	−10	.014	3.48	
L IPL	40	−56	−40	30	.030	5.97	1488
L FGmed	6	2	6	54	.026	5.42	1472
L Precentral Gyrus	4	−48	−4	52	.021	4.64	1088
R Insula	13	42	22	0	.021	4.60	1008
L Cingulate Gyrus	32	−2	22	42	.017	4.00	1000
L SFG	8	−4	24	48	.017	3.99	
L Anterior Nucleus (Thalamus)		−8	−8	10	.021	4.72	968
L Mammillary Body (Thalamus)		−10	−16	0	.014	3.49	
L MTG	37	−52	−56	2	.021	4.69	784
RBA45							
R MFG	46	50	30	14	.047	8.40	8224
R IFG	47	50	20	−6	.020	4.54	
R Insula	13	42	22	2	.016	4.00	
R Claustrum		34	22	−6	.014	3.58	
L MFG	46	−46	28	14	.022	4.84	5480
L IFG	44	−52	16	14	.021	4.77	
L MFG	9	−44	18	28	.020	4.51	
L Precentral Gyrus	6	−52	4	32	.014	3.50	
L IFG	46	−50	38	8	.013	3.33	
L Fusiform Gyrus	37	−44	−58	−16	.034	6.65	2712
L Claustrum		−32	20	2	.023	5.14	1152
L IPL	40	−42	−44	48	.021	4.83	936
L FGmed	32	0	16	48	.016	3.98	808
RFo6&7							
R IFG	47	40	36	−12	.042	8.00	4472
R IFG	46	50	34	6	.011	3.22	
L IFG	45	−52	28	10	.019	4.72	1816
L MFG	11	−44	38	−18	.014	3.82	
L IFG	47	−44	32	−12	.013	3.72	
L Fusiform Gyrus	37	−48	−54	−16	.021	5.06	792

Note: MNI coordinates correspond to cluster peaks. L: Left, R: Right, FGmed: Medial frontal gyrus, IFG: Inferior frontal gyrus, IPL: Inferior parietal lobule, ITG: Inferior temporal gyrus, MFG: Middle frontal gyrus, MTG: Middle temporal gyrus, SFG: Superior frontal gyrus, SPL: Superior parietal lobule, STG: Superior temporal gyrus.

defined IFG subdivisions (Xiang et al., 2010), which attributed this pattern of connectivity to inherent distinctions among the IFG subdivisions and their functional connections within the perisylvian language system. The involvement of LBA44 with a dorsal coactivation pattern and LBA45 and LFo6&7 with a ventral pattern is consistent with several neurocognitive models of language processing that emphasize ventral-dorsal disparity in the functional connectivity of Broca's area (Friederici, 2002, 2011, 2012; Hagoort, 2013, 2016; Hickok & Poeppel, 2004, 2007; Poeppel et al., 2012; Xiang et al., 2010). In general, these models implicate posterior-dorsal LIFG usually comprising LBA44, but sometimes also LBA45, with dorsal connections within the left frontal, temporal and sometimes parietal cortices, and the anterior-ventral LIFG usually comprising LBA47, but sometimes also LBA45, with ventral connections within the left frontal and temporal cortices. The functions attributed to the dorsal network range from syntactic processing (Friederici, 2002, 2011, 2012), syntactic and phonological processing (Hagoort, 2013, 2016; Xiang et al., 2010) to speech production (Hickok & Poeppel, 2004, 2007; Poeppel et al., 2012). On the other hand, the ventral network has been associated with semantic processing (Friederici, 2002, 2011, 2012; Hagoort, 2013, 2016; Xiang et al., 2010) and speech comprehension (Hickok & Poeppel, 2004, 2007; Poeppel et al., 2012). Given that the current study examined coactivation patterns of IFG subdivisions for language in general, but not for specific linguistic components, it is not possible to further characterize their functional roles.

In the left frontal lobe, LBA44 showed the greatest and most widespread coactivation, followed by LBA45 and finally by LFo6&7. Particularly, LBA44 and LBA45 coactivated with more extensive frontal regions spanning the inferior, middle and medial frontal gyri and the precentral gyrus as well as the insular cortex, whereas the coactivation of LFo6&7 was restricted largely to anterior-ventral frontal regions (middle and inferior frontal gyri), but also included the medial frontal gyrus. The coactivation of LIFG with the left dorsolateral prefrontal cortex and the dorsomedial prefrontal cortex including the anterior cingulate cortex is compatible with the Memory, Unification and Control (MUC) Model, which implicates these regions with executive control processes including attention and cognitive control underlying language (Hagoort, 2005, 2013, 2016; Xiang et al., 2010). Notably, as shown by the contrast analyses, LBA44 strongly coactivated with the superior-posterior part of the dorsolateral prefrontal cortex, while LBA45 strongly coactivated with the more anterior part. The coactivation results also related LFo6&7 with the inferior dorsolateral prefrontal cortex. Taken together, this ventral-anterior-posterior gradient within the dorsolateral prefrontal cortex (LBA46, 9 and 6) and its corresponding coactivation with ventral-anterior-posterior LIFG may represent the control processes underlying semantic, syntactic and phonological processes in parallel with the claims of the MUC Model (Hagoort, 2005, 2013, 2016; Xiang et al., 2010).

Of the left-hemispheric ROIs, only LBA44 coactivated with regions within the parietal lobe, specifically in the inferior parietal lobule (IPL) including the supramarginal gyrus and the superior parietal lobule (SPL) including the precuneus. The coactivation in SPL was bilateral, whereas that of IPL was found only in the left hemisphere. SPL is a functionally heterogenous region that has been bilaterally involved in various multisensory processes including action and visuomotor processing, visual perception, spatial cognition, reasoning, working memory, and attention (Wang, Yang, et al., 2015). IPL, on the other hand, has been more commonly implicated in language processing. Also known as Geschwind's territory (Catani, Jones, & Ffytche, 2005; Geschwind, 2006), left IPL was shown in DWT studies to indirectly connect Broca's and Wernicke's areas in parallel

with the arcuate fasciculus, which provides a direct pathway between the two (Catani et al., 2005). Various cognitive functions have been attributed to IPL including semantic processing (Catani et al., 2005), syntactic processing (Hagoort & Indefrey, 2014), reading and language learning (Barbeau et al., 2017), phonological storage as part of working memory (Baldo & Cronkers, 2006; Vigneau et al., 2006), number processing (Arsalidou & Taylor, 2011; Hung et al., 2015), processing tools and object-directed actions (Chen, Garcea, Jacobs, & Mahon, 2018), among others, stressing its role in various functional domains as a major network hub (Igelström & Graziano, 2017). According to the Dual-Stream Model of Speech Processing, the temporoparietal region at the posterior end of the sylvian fissure (area Spt) is part of the dorsal articulatory network together with dorsal LIFG (BA44 and 45), the left premotor cortex and the left insula, and is responsible for sensorimotor interface; i.e., translation of linguistic information between sensory (auditory, visual etc.) and production (motor) systems (Hickok & Poeppel, 2007; Poeppel et al., 2012). However, the IPL coactivation with LBA44 was observed more superiorly than area Spt; hence, it is not clear to what extent this coactivation converges with the functions attributed to area Spt. Coactivation of LBA44 and left IPL is also consistent with a recent version of Friederici's model of language processing, which argues for a second dorsal pathway connecting posterior STG with the premotor cortex, in addition to the primary dorsal pathway between LBA44 and posterior STG (Friederici, 2011, 2012). This second dorsal pathway is further divided into direct and indirect routes, the direct route connecting posterior STG directly with the premotor cortex, and the indirect route connecting posterior STG with the premotor cortex via the inferior parietal cortex. The premotor cortex in turn makes a loop with LBA44. It is argued that this second dorsal pathway facilitates mapping between phonological and motor/articulatory information. The coactivation of LBA44 with left IPL (supramarginal gyrus) is also consistent with the predictions of the MUC Model, which associates this connectivity with phonological processing (Hagoort, 2013, 2016; Xiang et al., 2010), given that left IPL is thought to be involved in phonological short-term memory. However, this model also predicts left parietal coactivations for LBA45 and LFo6&7 for syntactic and semantic processing, respectively, which were absent in the present study. Overall, these three neurocognitive models of language processing converge on the importance of the connection between the left inferior parietal cortex and dorsal LIFG for language processing, possibly for speech and phonology.

Within left temporal lobe, the coactivation networks of the three left-hemispheric ROIs converged in the posterior temporal lobe; specifically, on the posterior portion of the left middle temporal gyrus overlapping with portions of BA22; i.e., Wernicke's area. The contrast analyses, however, showed that only LFo6&7 strongly coactivated with parts of this posterior temporal region. The posterior superior and middle temporal lobe has been associated with various linguistic functions, primarily including phonological processing (particularly STG) (Turkeltaub & Branch Coslett, 2010; Vigneau et al., 2006), syntactic processing (Hagoort & Indefrey, 2014; Heard & Lee, 2020; Rodd et al., 2015; Vigneau et al., 2006; Walenski et al., 2019), semantic processing (Hagoort & Indefrey, 2014; Rodd et al., 2015; Vigneau et al., 2006), and sentence comprehension (Vigneau et al., 2006; Walenski et al., 2019). This multifunctional nature of the left posterior temporal lobe may have contributed to the present observation of convergent coactivation for all LIFG subdivisions in that area. Another region within the temporal lobe showing significant coactivation is the anterior middle temporal gyrus, which significantly coactivated only with LBA45. The anterior temporal lobe has been associated with sentence comprehension in an ALE meta-analysis (Walenski et al., 2019), and several neuroimaging studies implicated this region in combinatorial processing at the sentence level (higher syntactic and compositional semantic processing), usually identified through sentence versus word list contrasts (Brennan et al., 2012; Brennan & Pylkkänen, 2012; Bulut, Hung, Tzeng, & Wu, 2017; Colin Humphries, Love, Swinney, & Hickok, 2005; Humphries, Willard, Buchsbaum, & Hickok, 2001; Rogalsky & Hickok, 2009). The involvement of anterior MTG in sentence processing is consistent with the Dual-Stream Model, which associates the left anterior temporal lobe with combinatorial processing of syntactic and semantic information, and conceptualizes a direct connection between the ventral and dorsal streams via the left anterior temporal lobe and dorsal LIFG (LBA45, but also LBA44) (Hickok & Poeppel, 2004, 2007; Poeppel et al., 2012). LBA45 – left anterior temporal lobe coactivation is also compatible with Friederici's Model, according to which anterior STG, MTG and anterior IFG (BA45, but also BA47) constitute the ventral pathway underlying semantic processing (Friederici, 2002, 2011, 2012).

Another area that exhibited convergent coactivation for all left-hemispheric ROIs within the temporal lobe was the left fusiform gyrus. However, the contrast analyses showed that only LBA44 strongly coactivated with parts of this region. The left fusiform gyrus has been associated with reading and recognition of visual word forms (McCandliss, Cohen, & Dehaene, 2003), as well as with recognition of meaningful visual objects in general (Devlin, Jamison, Gonnerman, & Matthews, 2006). In particular, neuroimaging research as well as clinical studies of semantic dementia involved this region with lexical-semantic processing (Ardila, Bernal, & Rosselli, 2015; Binder, Desai, Graves, & Conant, 2009; Ding et al., 2016; Wheatley, Weisberg, Beauchamp, & Martin, 2005). The neurocognitive models of language processing do not explicitly associate the fusiform gyrus in the language network, except for involvement by the MUC Model of the LBA47 – left posterior inferior temporal gyrus connection with semantic processing (Hagoort, 2005, 2013, 2016). In the present study, though, the coactivation was within the fusiform gyrus, which is on the basal surface of the temporal lobe. Also, not only LFo6&7 corresponding to LBA47, but all three LIFG subdivisions significantly coactivated with the fusiform gyrus, contrary to the model's prediction of mainly LBA47 involvement with the left inferior temporal lobe.

Although LIFG ROIs revealed a strongly left-lateralized functional network, several right-hemispheric coactivations were also observed, especially for LBA44, to a lesser extent for LBA45, but none for LFo6&7. The right-hemispheric regions coactivating with both LBA44 and LBA45 include locations in the frontal lobe and the cingulate and insular cortices, while

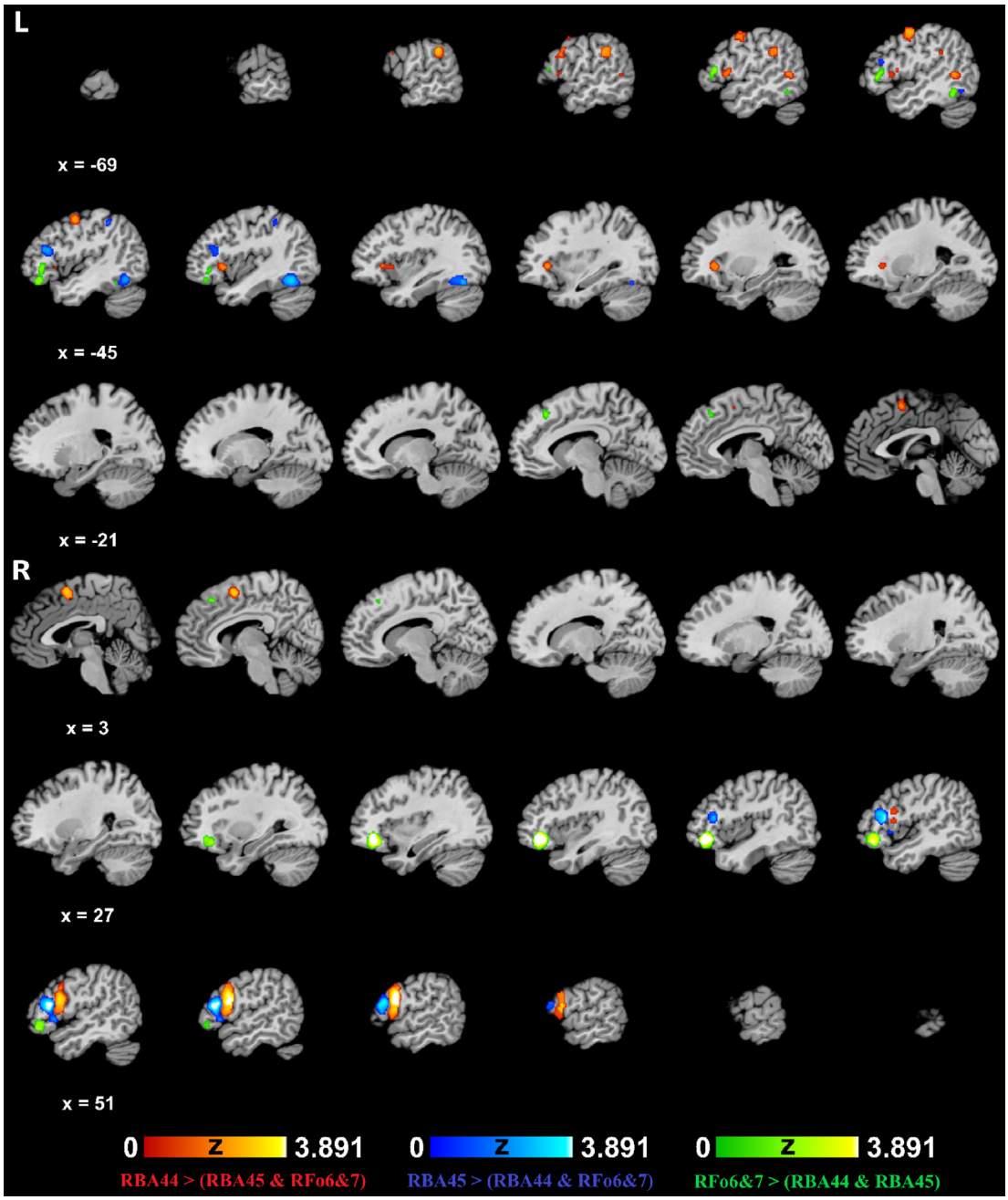

Fig. 5 – Contrast results for the right-hemispheric ROIs.

only LBA44 significantly coactivated with the right parietal cortex. Moreover, contrast analyses revealed that only LBA44 showed coactivation with right-hemispheric structures in the frontal lobe (MFG, SFG, precentral gyrus also spanning some homotopic RIFG territory), parietal lobe (precuneus) and the cingulate gyrus. Although it is difficult to characterize specific contributions of the right-hemispheric coactivations observed in the present study, they are unlikely to be merely due to contextual, prosodic and pragmatic processes, since the experiments included in the MACM analyses of LBA44 involved manipulations at various linguistic levels; i.e., speech, semantics, phonology, syntax and orthography. The language network generally proposed by neurocognitive models of language is strongly left-lateralized, with only limited involvement of the right hemisphere. Although the Dual-Stream Model recognizes some right-hemispheric contribution to language processing, it claims that only the ventral stream underlying speech comprehension involves bilateral temporal cortices, whereas the dorsal stream responsible for speech production is left dominant (Hickok & Poeppel, 2004, 2007; Poeppel et al., 2012). Therefore, the present finding of especially LBA44 coactivation within the right hemisphere challenges neurocognitive models of language processing that do not consider possible roles of the right hemisphere in the language network.

Table 6 – Contrast results for the right-hemispheric ROIs.

Anatomical label (Nearest gray matter within 5 mm)	BA	MNI coordinates			Z	Cluster size (mm^3)
		x	y	z		
RBA44 > (RBA45 & RFo6&7)						
R IFG	44	58.2	10.6	20	3.89	4856
R Precentral Gyrus	44	59	12	8	3.54	
L IPL	40	−62	−38	30	2.86	1056
L IPL	40	−62	−34	29	2.82	
L IPL	40	−52	−36	32	2.14	
R FGmed	6	7	4	56	3.12	1016
L Precentral Gyrus	4	−50	−2	54	2.69	984
L Precentral Gyrus	4	−50	−6	54	2.64	
L Precentral Gyrus	4	−52	−4	42	2.34	
L Insula		−42	16	−2	2.26	880
L IFG	45	−36	28	0	2.18	
L Claustrum		−26	26	0	2.12	
L ITG	37	−48	−56	2	2.31	408
L MTG	37	−52	−54	6	2.30	
L Precentral Gyrus	44	−52	10	8	2.08	296
L IFG	9	−58	14	26	1.91	208
L Precentral Gyrus	6	−58	10	34	1.90	
RBA45 > (RBA44 & RFo6&7)						
R IFG	45	52.6	25.6	13	3.89	3960
R IFG	45	52	20	−2	2.29	
L Declive (Cerebellum)		−38	−61	−16	3.35	1504
L Fusiform Gyrus	37	−38	−55	−14	3.24	
L MFG	46	−44	26	18	2.58	584
L MFG	46	−46	30	18	2.52	
L IPL	40	−46	−40	48	2.04	128
RFo6&7 > (RBA44 & RBA45)						
R IFG	47	39.6	36.9	−11.7	3.89	3936
L MFG	47	−42	38	−14	2.30	1072
L IFG	45	−54	28	8	2.26	
L IFG	13	−48	32	0	2.13	
L MFG	47	−44	36	−6	2.04	
L Culmen (Cerebellum)		−50	−52	−20	2.06	248
L Fusiform Gyrus	37	−52	−54	−16	2.05	
L FGmed	8	−8	32	44	2.37	200
R SFG	8	8	30	48	2.64	104

Note: MNI coordinates correspond to cluster peaks. L: Left, R: Right, FGmed: Medial frontal gyrus, IFG: Inferior frontal gyrus, IPL: Inferior parietal lobule, ITG: Inferior temporal gyrus, MFG: Middle frontal gyrus, MTG: Middle temporal gyrus, SFG: Superior frontal gyrus, SPL: Superior parietal lobule, STG: Superior temporal gyrus.

Previous research associated subcortical structures primarily including the thalamus and the basal ganglia with language; however, how these structures contribute to language processing and how they are connected to the language network remains to be elucidated (Friederici, 2012). In the present study, subcortical coactivations were seen exclusively for LBA44 in the thalamus, the basal ganglia (putamen) and the claustrum in the left hemisphere as part of a single cluster in the main coactivation analysis. This cluster predominantly included the thalamus (96.7%), while overlapping with fragments of the caudate body (1.9%) and the putamen (1.4%). Neuroimaging studies, animal models and neurodegenerative disorders of the basal ganglia including the caudate nucleus and the putamen associated this structure with various cognitive, motor and emotional processes particularly including reward processing, learning and memory, and motor control (Albin, Young, & Penney, 1989; Chakravarthy, Joseph, & Bapi, 2010; Groenewegen, 2003; Lanciego, Luquin, & Obeso, 2012; Packard & Knowlton, 2002). Indeed, the basal ganglia-thalamo-cortical system is associated with a wide spectrum of sensorimotor, cognitive, emotional and motivational brain functions (Alexander & Crutcher, 1990; Groenewegen, 2003). An MACM study of the left and right putamen coactivations in the domains of language and execution of speech also revealed that the left putamen exhibited a primarily left-lateralized coactivation network spanning regions associated with language processing (Viñas-Guasch & Wu, 2017). The authors implicated the left putamen particularly with semantic processes. The left caudate nucleus has also been associated with language processing, particularly learning a second language (Tan et al., 2011) and control processes in bilingualism such as code switching (Crinion et al., 2006; Zou, Ding, Abutalebi, Shu, & Peng, 2012), and lesions in the left caudate nucleus were shown to correlate with speech and language impairments following stroke, implicating this region in control processes involving speech and language (Grönholm, Roll, Horne, Sundgren, & Lindgren, 2016). In support of these associations, a DWT study identified a structural network involving the basal ganglia, the thalamus, and Broca's area, which is argued to support language processing (Ford et al., 2013). Specifically, the authors propose that this basal ganglia-thalamo-Broca's area system may facilitate semantic and lexical-phonological processes during word selection. Accordingly, the basal ganglia-thalamo-LBA44 circuit may support control processes in language processing.

Although all LIFG ROIs coactivated with parts of the cerebellum, the coactivation peaks for LBA45 and LFo6&7 were parts of a larger cluster in the left hemisphere involving the fusiform gyrus predominantly, but also the left cerebellum (declive) to a much lesser extent, while LBA44 coactivated with the right cerebellum (culmen) specifically. A previous MACM study identified similar coactivation in the culmen overlapping with a more robust cluster in the fusiform gyrus, which was attributed to imprecise allocation of activation in the culmen due to smoothing issues in preprocessing stages especially in adjacent lobes or structures (Bernal et al., 2015). Therefore, the cerebellar coactivation of LBA45 and LFo6&7 in the present study is dubious, whereas LBA44 reliably coactivated with the cerebellum. Indeed, the contrast analysis revealed that only LBA44 coactivated with the right cerebellum. The cerebellum has long been considered to underlie coordination of motor control, while particularly the right cerebellum has recently been associated with mediation of cognitive functions including language (Murdoch, 2010). Neuroimaging research implicated the right cerebellum in speech and language processing (Booth, Wood, Lu, Houk, & Bitan, 2007; Wildgruber, Ackermann, & Grodd, 2001). Also, children with specific language impairment and children with autism spectrum disorder accompanied by language impairment were shown to have morphological differences in the cerebellum compared to their typically developing peers (Hodge et al., 2010). Furthermore, a previous study reported increased activation in the right cerebellum when people with lesions in LBA44 engaged in speech production compared to

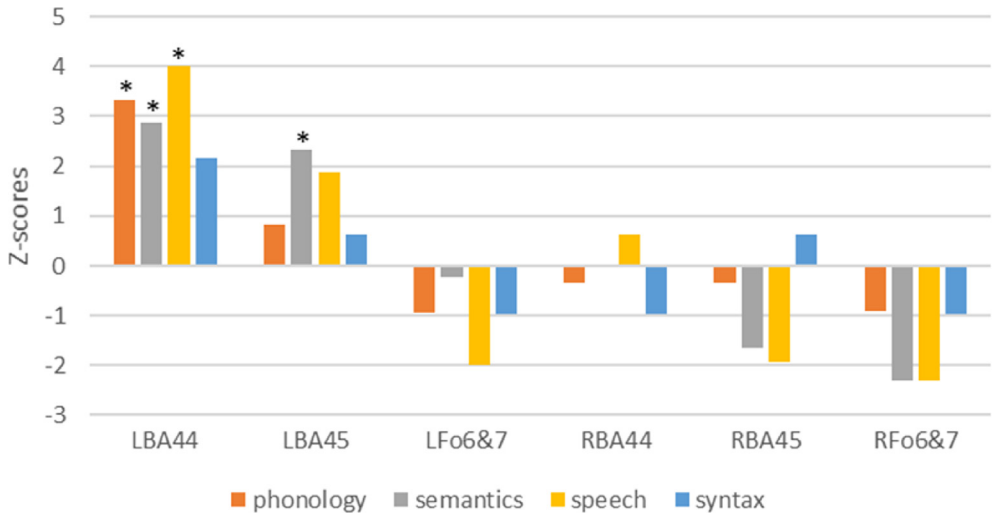

Fig. 6 – Functional decoding results for each ROI (* Bonferroni-corrected $p < .05$).

neurologically intact controls and patient controls with lesions elsewhere in the left hemisphere (Lorca-Puls et al., 2021). This activation was localized in a right cerebellar region very similar to the coactivation found in the current study and interpreted by the researchers as reflecting a compensatory function as part of a domain-general cognitive control mechanism during speech production. Moreover, a previous resting-state fMRI study revealed that Broca's and Wernicke's areas were functionally connected to the basal ganglia, the thalamus and the right cerebellum, which were argued to play a role in language processing (Tomasi & Volkow, 2012). The coactivation of LBA44 with the basal ganglia and the cerebellum is consistent with the Declarative/Procedural (DP) Model (Ullman, 2001, 2004, 2016), according to which the procedural system comprises the basal ganglia and the cerebellum, which are primarily involved in learning and consolidation of procedural memories, on the one hand, and the left premotor cortex (BA6) and posterior LIFG (BA44), which are claimed to process automatized procedural memories, on the other (Ullman, 2016). Specifically, some versions of the DP Model associates the right cerebellum with learning grammatical rules as well as searching lexical items in the declarative system (Ullman, 2001, 2004). Given that recent neuroscience research pointed to the importance of cerebello-basal ganglia-thalamo-cortical loop for motor and nonmotor functions (Bostan, Dum, & Strick, 2013; Bostan & Strick, 2010, 2018; Caligiore et al., 2017; Tomasi & Volkow, 2012), it is thought that the cerebellum may contribute to the basal ganglia-thalamo-LBA44 circuit discussed in the previous paragraph and may mediate and modulate cognitive functions including language (Murdoch, 2010).

4.2. *Coactivation patterns of right-hemispheric ROIs*

It was found that significantly more papers and experiments were identified for each left-hemispheric ROI compared to the right-hemispheric ones, and that each LIFG ROI showed more extensive coactivation than its homotopic RIFG counterpart. This is compatible with left-hemispheric dominance for language processing. Also, unlike LIFG ROIs, which revealed a mostly ipsilateral, left-lateralized coactivation network, RIFG ROIs coactivated mostly with contralateral, left-hemispheric regions. This suggests that while LIFG engages an intrahemispheric language network, RIFG involves an interhemispheric language circuitry, in line with previous investigations (Gotts et al., 2013; Vigneau et al., 2006, 2011). In parallel with the LIFG results, among RIFG ROIs, RBA44 and RBA45 revealed a more widespread coactivation pattern than RFo6&7. This finding suggests that there is functional segregation within RIFG as part of the language network similar to that of LIFG. Unlike LIFG ROIs, however, there was almost no overlap among all three RIFG ROIs in either the left or the right hemisphere, while RBA44 and RBA45 exhibited coactivation overlap in the left and right frontal and insular cortices. This lack of overlap in the coactivation network of all three RIFG subdivisions may constitute one of the functional characteristics that set this region apart from its left-hemispheric homologue and may reflect less consistent involvement in the literature of RIFG in language processing. Nevertheless, RIFG showed a coactivation pattern, somewhat similar to LIFG, within left frontal (IFG, MFG, precentral gyrus, medial frontal regions), insular, parietal (IPL) and temporal (MTG, fusiform gyrus) cortices, as well as subcortical regions (thalamus). This implies that the right hemisphere, particularly RIFG, takes part not only in contextual, holistic and prosodic aspects of language processing as commonly argued in the literature (Dara et al., 2014; George et al., 1996; Lundgren & Brownell, 2016; Parola et al., 2016; Patel et al., 2018; Stockbridge et al., 2021; Xu et al., 2005), but also in lower-level semantic, phonological, syntactic and speech-related processes in conjunction with the left hemisphere. However, given that the functional decoding analysis did not reveal any functional specificity for language subdomains within RIFG ROIs, that a disproportionately lower number of language-related studies were identified for RIFG ROIs than LIFG ROIs, and that both LIFG and RIFG ROIs coactivated mostly with left-hemispheric regions, the role of the right hemisphere in language processing seems to be rather limited.

In parallel with previous observations (Vigneau et al., 2011), it could be argued that the function of the right cerebral

hemisphere within the language network is not language-specific, but may relate to executive processes that are recruited in a task-dependent manner. Along similar lines, an fMRI study revealed that activation in several bilateral regions including IFG, MFG, the precentral gyrus and the insula increased as familiarity of the sentences read decreased (Lai, Van Dam, Conant, Binder, & Desai, 2015). The brain regions bilaterally associated in that study largely overlaps with the right and the left frontal regions coactivating with the RIFG ROIs in the present investigation. The authors of that study associated these right hemispheric regions particularly including right frontal and insular regions with increased cognitive demands of processing unfamiliar stimuli (Lai et al., 2015). Similarly, research on neuroimaging and neuromodulation in aphasia associated overactivation of the right hemisphere, specifically RIFG, with aphasia symptoms and highlighted its role in recovery from aphasia (Hartwigsen & Saur, 2019; Martin et al., 2009; Stefaniak et al., 2021), though it is controversial whether this is a compensatory mechanism or a maladaptive strategy (Torres et al., 2013; Turkeltaub, Coslett, et al., 2012). Furthermore, neuroscience research on aging revealed age-related reduction in functional asymmetry for various cognitive tasks including attention, working memory and inhibitory control (Dolcos, Rice, & Cabeza, 2002; Manan, Franz, Yusoff, & Mukari, 2013, 2014). Thus, when the current findings are interpreted in light of this previous research in healthy, clinical and aging populations, it is thought that the right hemisphere, and specifically RIFG, may support mainly left-lateralized language processes when additional cognitive resources are needed.

4.3. *Limitations*

Several potential limitations pertain to the present investigation and need addressing. First, the BrainMap database, from which the experiments coactivating with IFG ROIs were sampled in this study, represents only a subset of neuroimaging experiments on language processing. This is partially due to the criteria of inclusion in the database. To be eligible for inclusion in the database, published fMRI or PET experiments must report whole-brain coordinates in standard space (MNI or Talairach), which means that experiments reporting only region-of-interest or volume-of-interest results are excluded since they violate the assumption of random spatial distribution across the whole brain (Eickhoff et al., 2012; Müller et al., 2017, 2018). Nevertheless, BrainMap has been expanding continuously with addition of more neuroimaging research by the database staff and by independent researchers into the database, which ensures that it is an extensive and representative sample of neuroimaging studies. Indeed, at the time of the analysis, the functional database of BrainMap comprised 3406 papers corresponding to 16,901 experiments and 76,016 subjects. In addition, the number of language-related papers identified in the database and included in the MACM analyses was high for most of the ROIs particularly in the left hemisphere (72, 68 and 29 for LBA44, LBA45 and LFo6&7, respectively). However, the number of papers included in the MACM analyses of the right-hemispheric ROIs was lower (22, 21 and 14 for RBA44, RBA45 and RFo6&7, respectively). Of the right-hemispheric ROIs, only RFo6&7 was associated with a lower number of papers than the minimum (around 17–20 experiments) recommended for ALE meta-analyses to obtain enough power for detection of small effect sizes and to prevent over-influence of individual studies (Eickhoff et al., 2016; Müller et al., 2018). Therefore, the coactivation results concerning RFo6&7 should be interpreted cautiously.

Second, the lower number of language-related studies identified for the right-hemispheric ROIs may also be partially related with a potential publication bias against studies with involvement of mainly right-hemispheric regions in language processing and with null results for the left-hemisphere or specifically for LIFG. Similar biases have been shown for cognitive neuroscience and language research, for instance for sex-related differences in brain activation during language processing (Kaiser, Haller, Schmitz, & Nitsch, 2009) and for cognitive advantage associated with bilingualism (de Bruin, Treccani, & Della Sala, 2015). A potential publication bias favoring the left hemisphere and LIFG, in particular, would have been especially problematic if studies only with region of interest or volume of interest analyses without reporting whole-brain results were also included in the meta-analyses. However, given that the BrainMap database, from which studies in the present study were sampled, includes only experiments reporting whole-brain results, a potential publication bias against the right hemisphere stemming from brain coverage in statistical analyses is not likely. Nevertheless, beyond this technical aspect, it is difficult to rule out potential influences of a publication bias for LIFG on the current results altogether.

Third, the way the ROIs were defined clearly affects the experiments identified as a result of the database search and the connectivity results obtained. Although probabilistically defined opercular, triangular and orbital parts of IFG were used to define the subdivisions of Broca's area and its right-hemispheric homologue in the present study, recent research suggests greater functional heterogeneity within IFG beyond these anatomical subdivisions. For instance, several coactivation-based parcellation studies with functional decoding reported functionally distinct clusters within LBA44 and suggested further functional segregation of LBA44 into anterior and posterior regions, responsible for language and action, respectively, and each associated with differential functional networks (Clos et al., 2013; Papitto et al., 2020). A similar subdivision was also suggested for pars orbitalis (BA47) of LIFG in another study (Belyk et al., 2017), which associated lateral LBA47 with both semantic and emotional processing, and opercular LBA47 with emotional processing alone. Likewise, functional fractionation of RIFG has also been shown using similar techniques, suggesting, for instance, a posterior-to-anterior organization for action and cognition, respectively (Hartwigsen, Neef, Camilleri, Margulies, & Eickhoff, 2019). These observations align well with the association of LBA44 with multiple linguistic functions in the functional decoding analysis in the present study, revealing significant involvement in phonology, speech and semantics, and marginal involvement with syntax, implying that there may be functionally distinct clusters within this region. Nevertheless, the traditional subdivision of IFG into opercular, triangular and orbital parts remains pertinent to many theoretical models attempting to explain brain-language

associations (Friederici, 2002, 2011, 2012; Hagoort, 2005, 2013, 2016; Hickok & Poeppel, 2004, 2007; Poeppel et al., 2012; Ullman, 2001, 2004, 2016). Furthermore, the probabilistic atlas based on the brain's cytoarchitecture (Amunts et al., 2020) that was used in the current study to determine the ROIs allowed a more consistent characterization and localization anatomically (Robinson et al., 2010), and helped minimize variations between individual brains (Amunts et al., 2020; Fedorenko & Blank, 2020). Moreover, cytoarchitecture is closely associated with brain functions and connectivity patterns (Amunts et al., 2020; Goulas et al., 2018; Wojtasik et al., 2020). A further concern related to ROI definition applies to the orbital part of IFG (BA47), which was represented in the current study using combined Fo6 and Fo7 maps that spanned parts of the lateral orbitofrontal cortex primarily including BA47 (Wojtasik et al., 2020). This ROI definition, coupled with probabilistic thresholding, may have caused underrepresentation of the relevant anatomical region, which may partially explain the lack of an association between LBA47 and the language subdomains investigated in the functional decoding analysis. To illuminate a functionally segregated connectivity profile of IFG subdivisions underlying language, future research may look into the coactivation patterns of IFG subdivisions utilizing a more fine-grained parcellation approach such as multiple receptor mapping (Amunts et al., 2010), connectivity-based parcellation (Fan et al., 2016; Wang, Fan, et al., 2015) or coactivation-based parcellation (Clos et al., 2013; Hartwigsen et al., 2019).

Finally, the primary objective of the present research was to reveal coactivation patterns of IFG subdivisions for language in general, without specifically testing or contrasting involvement with particular language components (e.g., syntax, semantics, phonology, speech), tasks (e.g., comprehension, production), or stimulus presentation modalities (e.g., visual, auditory), which can influence brain-language associations. Addressing all these additional issues at the same time would be a tremendous initiative and surpass the bounds of a single study. Nevertheless, the present findings have been interpreted in relation to certain language components in light of previous research, though these interpretations should be approached tentatively. Future MACM studies may look into the coactivation patterns of LIFG subdivisions for different linguistic components such as syntax and semantics, which would further elucidate brain-language associations and enable a more specific test of neurocognitive models of language processing from a network perspective.

5. Conclusion

Utilizing the BrainMap functional database of neuroimaging experiments and meta-analytic connectivity modeling, the present investigation aimed to elucidate coactivation profiles of LIFG and RIFG subdivisions (pars opercularis/BA44, pars triangularis/BA45, and pars orbitalis/Fo6&7) during language tasks. A predominantly left-lateralized coactivation pattern was identified for both left- and right-hemispheric ROIs, underscoring the left-hemispheric dominance for language processing. Specifically, differences were revealed among the functional networks of LIFG subdivisions, with posterior-dorsal LIFG (BA44) coactivating with a more extensive dorsal network of regions, particularly spanning bilateral frontal, bilateral parietal, left temporal, left subcortical (thalamus and putamen), and right cerebellar regions, but anterior-ventral LIFG (BA45 and Fo6&7) showing an exclusively left-lateralized involvement of frontal and temporal regions. The findings highlight the extensive cortical and subcortical functional network underlying language and suggest functional segregation within LIFG, with LBA44 acting as a network hub with diverse cortical, subcortical and cerebellar connections as part of the language network. Overall, the present findings shed light on the functional circuitry of language and allowed scrutiny of the predictions made by neurocognitive models of language processing. Also, the functional circuitry of language identified here for healthy participants may also serve as a baseline against which the language network in clinical populations can be compared, potentially facilitating assessment of clinical outcomes in neurorehabilitation of language disorders such as aphasia.

Credit author statement

Talat Bulut: Conceptualization; methodology; software; data entry, analysis, validation and curation; writing, reviewing and editing; and visualization.

Funding

The author declares that no funds, grants, or other support were received during the preparation of this manuscript.

Data availability

The datasets analyzed and generated during the current study are available in the Mendeley Data repository, https://doi.org/10.17632/nyx2gz9yww.1.

Open practices

The study in this article earned an Open Data – Protected Access badge for transparent practices. Materials and data for the study are available at https://doi.org/10.17632/nyx2gz9yww.1.

Declaration of competing interest

The author has no relevant financial or non-financial interests to disclose.

REFERENCES

Albin, R. L., Young, A. B., & Penney, J. B. (1989). The functional anatomy of basal ganglia disorders. *Trends in Neurosciences, 12*(10). https://doi.org/10.1016/0166-2236(89)90074-X

Alexander, G. E., & Crutcher, M. D. (1990). Functional architecture of basal ganglia circuits: Neural substrates of parallel processing. *Trends in Neurosciences, 13*(7), 266–271. https://doi.org/10.1016/0166-2236(90)90107-L

Amunts, K., Lenzen, M., Friederici, A. D., Schleicher, A., Morosan, P., Palomero-Gallagher, N., & Zilles, K. (2010). Broca's region: Novel organizational principles and multiple receptor mapping. *PLoS Biology, 8*(9), Article e1000489. https://doi.org/10.1371/journal.pbio.1000489

Amunts, K., Mohlberg, H., Bludau, S., & Zilles, K. (2020). Julich-Brain: A 3D probabilistic atlas of the human brain's cytoarchitecture. *Science, 369*(6506), 988–992. https://doi.org/10.1126/science.abb4588

Amunts, K., Schleicher, A., Bürgel, U., Mohlberg, H., Uylings, H. B. M., & Zilles, K. (1999). Broca's region revisited: Cytoarchitecture and intersubject variability. *The Journal of Comparative Neurology, 412*(2), 319–341. https://doi.org/10.1002/(SICI)1096-9861(19990920)412:2<319::AID-CNE10>3.0.CO;2-7

Ardila, A., Bernal, B., & Rosselli, M. (2015). Language and visual perception associations: Meta-analytic connectivity modeling of Brodmann area 37. *Behavioural Neurology, 2015*, 1–14. https://doi.org/10.1155/2015/565871

Ardila, A., Bernal, B., & Rosselli, M. (2016). How extended is Wernicke's area? Meta-analytic connectivity study of BA20 and integrative proposal. *Neuroscience Journal, 2016*, 1–6. https://doi.org/10.1155/2016/4962562

Arsalidou, M., & Taylor, M. J. (2011). Is 2+2=4? Meta-analyses of brain areas needed for numbers and calculations. *NeuroImage, 54*(3), 2382–2393. https://doi.org/10.1016/j.neuroimage.2010.10.009

Baldo, J. V., & Cronkers, N. F. (2006). The role of inferior parietal and inferior frontal cortex in working memory. *Neuropsychology, 20*(5). https://doi.org/10.1037/0894-4105.20.5.529

Barbeau, E. B., Chai, X. J., Chen, J.-K., Soles, J., Berken, J., Baum, S., … Klein, D. (2017). The role of the left inferior parietal lobule in second language learning: An intensive language training fMRI study. *Neuropsychologia, 98*, 169–176. https://doi.org/10.1016/j.neuropsychologia.2016.10.003 (August 2016).

Belyk, M., Brown, S., Lim, J., & Kotz, S. A. (2017). Convergence of semantics and emotional expression within the IFG pars orbitalis. *NeuroImage, 156*, 240–248. https://doi.org/10.1016/j.neuroimage.2017.04.020 (January).

Bernal, B., Ardila, A., & Rosselli, M. (2015). Broca's area network in language function: A pooling-data connectivity study. *Frontiers in Psychology, 6*, 1–8. https://doi.org/10.3389/fpsyg.2015.00687 (May).

Binder, J. R., Desai, R. H., Graves, W. W., & Conant, L. L. (2009). Where is the semantic system? A critical review and meta-analysis of 120 functional neuroimaging studies. *Cerebral Cortex, 19*(12). https://doi.org/10.1093/cercor/bhp055

Booth, J. R., Wood, L., Lu, D., Houk, J. C., & Bitan, T. (2007). The role of the basal ganglia and cerebellum in language processing. *Brain Research, 1133*(1). https://doi.org/10.1016/j.brainres.2006.11.074

Bostan, A. C., Dum, R. P., & Strick, P. L. (2013). Cerebellar networks with the cerebral cortex and basal ganglia. *Trends in Cognitive Sciences, 17*(5), 241–254. https://doi.org/10.1016/j.tics.2013.03.003

Bostan, A. C., & Strick, P. L. (2010). The cerebellum and basal ganglia are interconnected. *Neuropsychology Review, 20*(3), 261–270. https://doi.org/10.1007/s11065-010-9143-9

Bostan, A. C., & Strick, P. L. (2018). The basal ganglia and the cerebellum: Nodes in an integrated network. *Nature Reviews Neuroscience, 19*(6), 338–350. https://doi.org/10.1038/s41583-018-0002-7

Bozic, M., Fonteneau, E., Su, L., & Marslen-Wilson, W. D. (2015). Grammatical analysis as a distributed neurobiological function. *Human Brain Mapping, 36*(3), 1190–1201. https://doi.org/10.1002/hbm.22696

Brennan, J., Nir, Y., Hasson, U., Malach, R., Heeger, D. J., & Pylkkänen, L. (2012). Syntactic structure building in the anterior temporal lobe during natural story listening. *Brain and Language, 120*(2). https://doi.org/10.1016/j.bandl.2010.04.002

Brennan, J., & Pylkkänen, L. (2012). The time-course and spatial distribution of brain activity associated with sentence processing. *NeuroImage, 60*(2), 1139–1148. https://doi.org/10.1016/j.neuroimage.2012.01.030

Bulut, T. (2022). Neural correlates of morphological processing: An activation likelihood estimation meta-analysis. *Cortex*. https://doi.org/10.1016/j.cortex.2022.02.010

Bulut, T., Hung, Y.-H., Tzeng, O., & Wu, D. H. (2017). Neural correlates of processing sentences and compound words in Chinese. *PLoS One, 12*(12), Article e0188526. https://doi.org/10.1371/journal.pone.0188526

Caligiore, D., Pezzulo, G., Baldassarre, G., Bostan, A. C., Strick, P. L., Doya, K., … Herreros, I. (2017). Consensus paper: Towards a systems-level view of cerebellar function: The interplay between cerebellum, basal ganglia, and cortex. *The Cerebellum, 16*(1), 203–229. https://doi.org/10.1007/s12311-016-0763-3

Cardillo, E. R., McQuire, M., & Chatterjee, A. (2018). Selective metaphor impairments after left, not right, hemisphere injury. *Frontiers in Psychology, 9*. https://doi.org/10.3389/fpsyg.2018.02308. Dec.

Catani, M., Jones, D. K., & Ffytche, D. H. (2005). Perisylvian language networks of the human brain. *Annals of Neurology, 57*(1), 8–16. https://doi.org/10.1002/ana.20319

Chakravarthy, V. S., Joseph, D., & Bapi, R. S. (2010). What do the basal ganglia do? A modeling perspective. *Biological Cybernetics*. https://doi.org/10.1007/s00422-010-0401-y

Chen, Q., Garcea, F. E., Jacobs, R. A., & Mahon, B. Z. (2018). Abstract representations of object-directed action in the left inferior parietal lobule. *Cerebral Cortex, 28*(6). https://doi.org/10.1093/cercor/bhx120

Cieslik, E. C., Mueller, V. I., Eickhoff, C. R., Langner, R., & Eickhoff, S. B. (2015). Three key regions for supervisory attentional control: Evidence from neuroimaging meta-analyses. *Neuroscience and Biobehavioral Reviews, 48*, 22–34. https://doi.org/10.1016/j.neubiorev.2014.11.003

Clos, M., Amunts, K., Laird, A. R., Fox, P. T., & Eickhoff, S. B. (2013). Tackling the multifunctional nature of Broca's region meta-analytically: Co-activation-based parcellation of area 44. *NeuroImage, 83*, 174–188. https://doi.org/10.1016/j.neuroimage.2013.06.041

Crinion, J., Turner, R., Grogan, A., Hanakawa, T., Noppeney, U., Devlin, J. T., … Price, C. J. (2006). Language control in the bilingual brain. *Science, 312*(5779). https://doi.org/10.1126/science.1127761

Dapretto, M., & Bookheimer, S. Y. (1999). Form and content: Dissociating syntax and semantics in sentence comprehension. *Neuron, 24*(2), 427–432. https://doi.org/10.1016/S0896-6273(00)80855-7

Dara, C., Bang, J., Gottesman, R. F., & Hillis, A. E. (2014). Right hemisphere dysfunction is better predicted by emotional prosody impairments as compared to neglect. *Journal of Neurology & Translational Neuroscience, 2*(1).

D'Astolfo, L., & Rief, W. (2017). Learning about expectation violation from prediction error paradigms – A meta-analysis on brain processes following a prediction error. *Frontiers in Psychology, 8*, 1–11. https://doi.org/10.3389/fpsyg.2017.01253 (July).

de Bruin, A., Treccani, B., & Della Sala, S. (2015). Cognitive advantage in bilingualism. *Psychological Science, 26*(1), 99–107. https://doi.org/10.1177/0956797614557866

Devlin, J. T., Jamison, H. L., Gonnerman, L. M., & Matthews, P. M. (2006). The role of the posterior fusiform gyrus in reading. *Journal of Cognitive Neuroscience, 18*(6). https://doi.org/10.1162/jocn.2006.18.6.911

Devlin, J. T., Matthews, P. M., & Rushworth, M. F. S. (2003). Semantic processing in the left inferior prefrontal cortex: A combined functional magnetic resonance imaging and transcranial magnetic stimulation study. *Journal of Cognitive Neuroscience, 15*(1), 71–84. https://doi.org/10.1162/089892903321107837

Ding, J., Chen, K., Chen, Y., Fang, Y., Yang, Q., Lv, Y., … Han, Z. (2016). The left fusiform gyrus is a critical region contributing to the core behavioral profile of semantic dementia. *Frontiers in Human Neuroscience, 10*. https://doi.org/10.3389/fnhum.2016.00215 (May 2016).

Dolcos, F., Rice, H. J., & Cabeza, R. (2002). Hemispheric asymmetry and aging: Right hemisphere decline or asymmetry reduction. *Neuroscience and Biobehavioral Reviews, 26*(7), 819–825. https://doi.org/10.1016/S0149-7634(02)00068-4

Eickhoff, S. B., Bzdok, D., Laird, A. R., Kurth, F., & Fox, P. T. (2012). Activation likelihood estimation meta-analysis revisited. *NeuroImage, 59*(3), 2349–2361. https://doi.org/10.1016/j.neuroimage.2011.09.017

Eickhoff, S. B., Bzdok, D., Laird, A. R., Roski, C., Caspers, S., Zilles, K., & Fox, P. T. (2011). Co-activation patterns distinguish cortical modules, their connectivity and functional differentiation. *NeuroImage, 57*(3), 938–949. https://doi.org/10.1016/j.neuroimage.2011.05.021

Eickhoff, S. B., Laird, A. R., Grefkes, C., Wang, L. E., Zilles, K., & Fox, P. T. (2009). Coordinate-based activation likelihood estimation meta-analysis of neuroimaging data: A random-effects approach based on empirical estimates of spatial uncertainty. *Human Brain Mapping, 30*(9), 2907–2926. https://doi.org/10.1002/hbm.20718

Eickhoff, S. B., Nichols, T. E., Laird, A. R., Hoffstaedter, F., Amunts, K., Fox, P. T., … Eickhoff, C. R. (2016). Behavior, sensitivity, and power of activation likelihood estimation characterized by massive empirical simulation. *NeuroImage, 137*, 70–85. https://doi.org/10.1016/j.neuroimage.2016.04.072

Erickson, L. C., Rauschecker, J. P., & Turkeltaub, P. E. (2017). Meta-analytic connectivity modeling of the human superior temporal sulcus. *Brain Structure & Function, 222*(1), 267–285. https://doi.org/10.1007/s00429-016-1215-z

Fan, L., Li, H., Zhuo, J., Zhang, Y., Wang, J., Chen, L., … Jiang, T. (2016). The human Brainnetome Atlas: A new brain atlas based on connectional architecture. *Cerebral Cortex, 26*(8), 3508–3526. https://doi.org/10.1093/cercor/bhw157

Fedorenko, E., & Blank, I. A. (2020). Broca's area is not a natural kind. *Trends in Cognitive Sciences, 24*(4), 270–284. https://doi.org/10.1016/j.tics.2020.01.001

Fedorenko, E., Duncan, J., & Kanwisher, N. (2012). Language-selective and domain-general regions lie side by side within Broca's area. *Current Biology, 22*(21), 2059–2062. https://doi.org/10.1016/j.cub.2012.09.011

Ford, A. A., Triplett, W., Sudhyadhom, A., Gullett, J., McGregor, K., FitzGerald, D. B., … Crosson, B. (2013 May). Broca's area and its striatal and thalamic connections: A diffusion-MRI tractography study. *Frontiers in Neuroanatomy, 7*. https://doi.org/10.3389/fnana.2013.00008

Fox, P. T., Laird, A. R., Fox, S. P., Fox, P. M., Uecker, A. M., Crank, M., … Lancaster, J. L. (2005). Brainmap taxonomy of experimental design: Description and evaluation. *Human Brain Mapping, 25*(1), 185–198. https://doi.org/10.1002/hbm.20141

Fox, P. T., & Lancaster, J. L. (2002). Mapping context and content: The BrainMap model. *Nature Reviews Neuroscience, 3*(4), 319–321. https://doi.org/10.1038/nrn789

Friederici, A. D. (2002). Towards a neural basis of auditory sentence processing. *Trends in Cognitive Sciences, 6*(2), 78–84. https://doi.org/10.1016/S1364-6613(00)01839-8

Friederici, A. D. (2011). The brain basis of language processing: From structure to function. *Physiological Reviews, 91*(4), 1357–1392. https://doi.org/10.1152/physrev.00006.2011

Friederici, A. D. (2012). The cortical language circuit: From auditory perception to sentence comprehension. *Trends in Cognitive Sciences, 16*(5), 262–268. https://doi.org/10.1016/j.tics.2012.04.001

Gainotti, G. (2016). Lower- and higher-level models of right hemisphere language. A selective survey. *Functional Neurology, 31*(2). https://doi.org/10.11138/FNeur/2016.31.2.067

Galletta, E. E., Rao, P. R., & Barrett, A. M. (2011). Transcranial magnetic stimulation (TMS): Potential progress for language improvement in aphasia. *Topics in Stroke Rehabilitation, 18*(2), 87–91. https://doi.org/10.1310/tsr1802-87

Garrison, J., Erdeniz, B., & Done, J. (2013). Prediction error in reinforcement learning: A meta-analysis of neuroimaging studies. *Neuroscience and Biobehavioral Reviews, 37*(7), 1297–1310. https://doi.org/10.1016/j.neubiorev.2013.03.023

George, M. S., Parekh, P. I., Rosinsky, N., Ketter, T. A., Kimbrell, T. A., Heilman, K. M., … Post, R. M. (1996). Understanding emotional prosody activates right hemisphere regions. *Archives of Neurology, 53*(7). https://doi.org/10.1001/archneur.1996.00550070103017

Geschwind, N. (2006). The organization of language and the brain (1970). In *Broca's region* (Vol. 170, pp. 376–382). Oxford University Press. https://doi.org/10.1093/acprof:oso/9780195177640.003.0026.

Gitelman, D. R., Nobre, A. C., Sonty, S., Parrish, T. B., & Mesulam, M.-M. (2005). Language network specializations: An analysis with parallel task designs and functional magnetic resonance imaging. *NeuroImage, 26*(4), 975–985. https://doi.org/10.1016/j.neuroimage.2005.03.014

Glasser, M. F., & Rilling, J. K. (2008). DTI tractography of the human brain's language pathways. *Cerebral Cortex, 18*(11), 2471–2482. https://doi.org/10.1093/cercor/bhn011

Gotts, S. J., Jo, H. J., Wallace, G. L., Saad, Z. S., Cox, R. W., & Martin, A. (2013). Two distinct forms of functional lateralization in the human brain. *Proceedings of the National Academy of Sciences, 110*(36), 3435–3444. https://doi.org/10.1073/pnas.1302581110

Goulas, A., Zilles, K., & Hilgetag, C. C. (2018). Cortical gradients and laminar projections in mammals. *Trends in Neurosciences, 41*(11), 775–788. https://doi.org/10.1016/j.tins.2018.06.003

Grodzinsky, Y., Pieperhoff, P., & Thompson, C. (2021). Stable brain loci for the processing of complex syntax: A review of the current neuroimaging evidence. *Cortex, 142*, 252–271. https://doi.org/10.1016/j.cortex.2021.06.003

Groenewegen, H. J. (2003). The basal ganglia and motor control. *Neural Plasticity, 10*(1–2), 107–120. https://doi.org/10.1155/NP.2003.107

Grönholm, E. O., Roll, M. C., Horne, M. A., Sundgren, P. C., & Lindgren, A. G. (2016). Predominance of caudate nucleus lesions in acute ischaemic stroke patients with impairment in language and speech. *European Journal of Neurology, 23*(1). https://doi.org/10.1111/ene.12822

Hagoort, P. (2005). On Broca, brain, and binding: A new framework. *Trends in Cognitive Sciences, 9*(9), 416–423. https://doi.org/10.1016/j.tics.2005.07.004

Hagoort, P. (2013). MUC (Memory, Unification, Control) and beyond. *Frontiers in Psychology, 4*, 1–13. https://doi.org/10.3389/fpsyg.2013.00416 (July).

Hagoort, P. (2016). MUC (Memory, Unification, Control). In *Neurobiology of language* (pp. 339–347). Elsevier. https://doi.org/10.1016/B978-0-12-407794-2.00028-6.

Hagoort, P., & Indefrey, P. (2014). The neurobiology of language beyond single words. *Annual Review of Neuroscience, 37*(1), 347–362. https://doi.org/10.1146/annurev-neuro-071013-013847

Hartwigsen, G., Neef, N. E., Camilleri, J. A., Margulies, D. S., & Eickhoff, S. B. (2019). Functional segregation of the right inferior frontal gyrus: Evidence from coactivation-based parcellation. *Cerebral Cortex, 29*(4), 1532–1546. https://doi.org/10.1093/cercor/bhy049

Hartwigsen, G., & Saur, D. (2019). Neuroimaging of stroke recovery from aphasia – Insights into plasticity of the human language network. *NeuroImage, 190*, 14–31. https://doi.org/10.1016/j.neuroimage.2017.11.056 (November 2017).

Heard, M., & Lee, Y. S. (2020). Shared neural resources of rhythm and syntax: An ALE meta-analysis. *Neuropsychologia, 137*, Article 107284. https://doi.org/10.1016/j.neuropsychologia.2019.107284 (November 2019).

Heim, S., Opitz, B., Müller, K., & Friederici, A. D. (2003). Phonological processing during language production: fMRI evidence for a shared production-comprehension network. *Cognitive Brain Research, 16*(2), 285–296. https://doi.org/10.1016/S0926-6410(02)00284-7

Hickok, G., & Poeppel, D. (2004). Dorsal and ventral streams: A framework for understanding aspects of the functional anatomy of language. *Cognition, 92*(1–2), 67–99. https://doi.org/10.1016/j.cognition.2003.10.011

Hickok, G., & Poeppel, D. (2007). The cortical organization of speech processing. *Nature Reviews Neuroscience, 8*(5), 393–402. https://doi.org/10.1038/nrn2113

Hobeika, L., Diard-Detoeuf, C., Garcin, B., Levy, R., & Volle, E. (2016). General and specialized brain correlates for analogical reasoning: A meta-analysis of functional imaging studies. *Human Brain Mapping, 37*(5), 1953–1969. https://doi.org/10.1002/hbm.23149

Hodge, S. M., Makris, N., Kennedy, D. N., Caviness, V. S., Howard, J., McGrath, L., … Harris, G. J. (2010). Cerebellum, language, and cognition in autism and specific language impairment. *Journal of Autism and Developmental Disorders, 40*(3). https://doi.org/10.1007/s10803-009-0872-7

Hoffman, P., & Morcom, A. M. (2018). Age-related changes in the neural networks supporting semantic cognition: A meta-analysis of 47 functional neuroimaging studies. *Neuroscience and Biobehavioral Reviews, 84*, 134–150. https://doi.org/10.1016/j.neubiorev.2017.11.010 (November 2017).

Holland, R., & Crinion, J. (2012). Can tDCS enhance treatment of aphasia after stroke? *Aphasiology, 26*(9), 1169–1191. https://doi.org/10.1080/02687038.2011.616925

Hummel, F. C., & Cohen, L. G. (2006). Non-invasive brain stimulation: A new strategy to improve neurorehabilitation after stroke? *The Lancet Neurology, 5*(8), 708–712. https://doi.org/10.1016/S1474-4422(06)70525-7

Humphries, C., Love, T., Swinney, D., & Hickok, G. (2005). Response of anterior temporal cortex to syntactic and prosodic manipulations during sentence processing. *Human Brain Mapping, 26*(2), 128–138. https://doi.org/10.1002/hbm.20148

Humphries, C., Willard, K., Buchsbaum, B., & Hickok, G. (2001). Role of anterior temporal cortex in auditory sentence comprehension: An fMRI study. *Neuroreport, 12*(8), 1749–1752.

Hung, Y.-H., Pallier, C., Dehaene, S., Lin, Y.-C., Chang, A., Tzeng, O. J.-L., & Wu, D. H. (2015). Neural correlates of merging number words. *NeuroImage, 122*, 33–43. https://doi.org/10.1016/j.neuroimage.2015.07.045

Igelström, K. M., & Graziano, M. S. A. (2017). The inferior parietal lobule and temporoparietal junction: A network perspective. *Neuropsychologia, 105*. https://doi.org/10.1016/j.neuropsychologia.2017.01.001

Kaiser, A., Haller, S., Schmitz, S., & Nitsch, C. (2009). On sex/gender related similarities and differences in fMRI language research. *Brain Research Reviews, 61*(2), 49–59. https://doi.org/10.1016/j.brainresrev.2009.03.005

Klimovich-Gray, A., & Bozic, M. (2019). Domain-general and domain-specific computations in single word processing. *NeuroImage, 202*, Article 116112. https://doi.org/10.1016/j.neuroimage.2019.116112 (June).

Kollndorfer, K., Krajnik, J., Woitek, R., Freiherr, J., Prayer, D., & Schöpf, V. (2013). Altered likelihood of brain activation in attention and working memory networks in patients with multiple sclerosis: An ALE meta-analysis. *Neuroscience and Biobehavioral Reviews, 37*(10), 2699–2708. https://doi.org/10.1016/j.neubiorev.2013.09.005

Laine, M., Rinne, J. O., Krause, B. J., Teräs, M., & Sipilä, H. (1999). Left hemisphere activation during processing of morphologically complex word forms in adults. *Neuroscience Letters, 271*(2), 85–88. https://doi.org/10.1016/S0304-3940(99)00527-3

Laird, A. R., Lancaster, J. L., & Fox, P. T. (2005). BrainMap: The social evolution of a human brain mapping database. *Neuroinformatics, 3*(1), 65–78. https://doi.org/10.1385/NI:3:1:065

Laird, A. R., Robinson, J. L., McMillan, K. M., Tordesillas-Gutiérrez, D., Moran, S. T., Gonzales, S. M., … Lancaster, J. L. (2010). Comparison of the disparity between Talairach and MNI coordinates in functional neuroimaging data: Validation of the Lancaster transform. *NeuroImage, 51*(2), 677–683. https://doi.org/10.1016/j.neuroimage.2010.02.048

Lai, V. T., Van Dam, W., Conant, L. L., Binder, J. R., & Desai, R. H. (2015). Familiarity differentially affects right hemisphere contributions to processing metaphors and literals. *Frontiers in Human Neuroscience, 9*. https://doi.org/10.3389/fnhum.2015.00044 (Feb).

Lancaster, J. L., Cykowski, M. D., McKay, D. R., Kochunov, P. V., Fox, P. T., Rogers, W., … Mazziotta, J. (2010). Anatomical global spatial normalization. *Neuroinformatics, 8*(3), 171–182. https://doi.org/10.1007/s12021-010-9074-x

Lancaster, J. L., Laird, A. R., Eickhoff, S. B., Martinez, M. J., Fox, P. M., & Fox, P. T. (2012). Automated regional behavioral analysis for human brain images. *Frontiers in Neuroinformatics, 6*, 1–12. https://doi.org/10.3389/fninf.2012.00023 (July 2012).

Lancaster, J. L., Rainey, L. H., Summerlin, J. L., Freitas, C. S., Fox, P. T., Evans, A. C., … Mazziotta, J. C. (1997). Automated labeling of the human brain: A preliminary report on the development and evaluation of a forward-transform method. *Human Brain Mapping, 5*(4), 238–242. https://doi.org/10.1002/(SICI)1097-0193(1997)5:4<238::AID-HBM6>3.0.CO;2-4

Lancaster, J. L., Tordesillas-Gutiérrez, D., Martinez, M., Salinas, F., Evans, A., Zilles, K., … Fox, P. T. (2007). Bias between MNI and Talairach coordinates analyzed using the ICBM-152 brain template. *Human Brain Mapping, 28*(11), 1194–1205. https://doi.org/10.1002/hbm.20345

Lancaster, J. L., Woldorff, M. G., Parsons, L. M., Liotti, M., Freitas, C. S., Rainey, L., … Fox, P. T. (2000). Automated Talairach Atlas labels for functional brain mapping. *Human Brain Mapping, 10*(3), 120–131. https://doi.org/10.1002/1097-0193(200007)10:3<120::AID-HBM30>3.0.CO;2-8

Lanciego, J. L., Luquin, N., & Obeso, J. A. (2012). Functional neuroanatomy of the basal ganglia. *Cold Spring Harbor Perspectives in Medicine, 2*(12). https://doi.org/10.1101/cshperspect.a009621

Lefaucheur, J.-P., Antal, A., Ayache, S. S., Benninger, D. H., Brunelin, J., Cogiamanian, F., … Paulus, W. (2017). Evidence-based guidelines on the therapeutic use of transcranial direct current stimulation (tDCS). *Clinical Neurophysiology, 128*(1), 56–92. https://doi.org/10.1016/j.clinph.2016.10.087

Lorca-Puls, D. L., Gajardo-Vidal, A., Oberhuber, M., Prejawa, S., Hope, T. M. H., Leff, A. P., … Price, C. J. (2021). Brain regions that support accurate speech production after damage to

Broca's area. *Brain Communications, 3*(4), 1–19. https://doi.org/10.1093/braincomms/fcab230

Lundgren, K., & Brownell, H. (2016). Figurative language deficits associated with right hemisphere disorder. *Perspectives of the ASHA Special Interest Groups, 1*(2). https://doi.org/10.1044/persp1.sig2.66

Lundgren, K., Brownell, H., Cayer-Meade, C., Milione, J., & Kearns, K. (2011). Treating metaphor interpretation deficits subsequent to right hemisphere brain damage: Preliminary results. *Aphasiology, 25*(4). https://doi.org/10.1080/02687038.2010.500809

Maess, B., Koelsch, S., Gunter, T. C., & Friederici, A. D. (2001). Musical syntax is processed in Broca's area: An MEG study. *Nature Neuroscience, 4*(5), 540–545. https://doi.org/10.1038/87502

Manan, H. A., Franz, E. A., Yusoff, A. N., & Mukari, S. Z.-M. S. (2013). Age-related laterality shifts in auditory and attention networks with normal ageing: Effects on a working memory task. *Neurology, Psychiatry and Brain Research, 19*(4), 180–191. https://doi.org/10.1016/j.npbr.2013.09.001

Manan, H. A., Franz, E. A., Yusoff, A. N., & Mukari, S. Z.-M. S. (2014). Age-related brain activation during forward and backward verbal memory tasks. *Neurology, Psychiatry and Brain Research, 20*(4), 76–86. https://doi.org/10.1016/j.npbr.2014.08.001

Martin, P. I., Naeser, M. A., Ho, M., Doron, K. W., Kurland, J., Kaplan, J., … Pascual-Leone, A. (2009). Overt naming fMRI pre- and post-TMS: Two nonfluent aphasia patients, with and without improved naming post-TMS. *Brain and Language, 111*(1), 20–35. https://doi.org/10.1016/j.bandl.2009.07.007

Maruyama, M., Pallier, C., Jobert, A., Sigman, M., & Dehaene, S. (2012). The cortical representation of simple mathematical expressions. *NeuroImage, 61*(4), 1444–1460. https://doi.org/10.1016/j.neuroimage.2012.04.020

Matsuo, K., Chen, S.-H. A., Hue, C.-W., Wu, C.-Y., Bagarinao, E., Tseng, W.-Y. I., & Nakai, T. (2010). Neural substrates of phonological selection for Japanese character Kanji based on fMRI investigations. *NeuroImage, 50*(3), 1280–1291. https://doi.org/10.1016/j.neuroimage.2009.12.099

McCandliss, B. D., Cohen, L., & Dehaene, S. (2003). The visual word form area: Expertise for reading in the fusiform gyrus. *Trends in Cognitive Sciences, 7*(7), 293–299. https://doi.org/10.1016/S1364-6613(03)00134-7

McDermott, K. B., Petersen, S. E., Watson, J. M., & Ojemann, J. G. (2003). A procedure for identifying regions preferentially activated by attention to semantic and phonological relations using functional magnetic resonance imaging. *Neuropsychologia, 41*(3), 293–303. https://doi.org/10.1016/S0028-3932(02)00162-8

Meyer, L., & Friederici, A. D. (2016). Neural systems underlying the processing of complex sentences. In *Neurobiology of language* (pp. 597–606). Elsevier. https://doi.org/10.1016/B978-0-12-407794-2.00048-1.

Müller, V. I., Cieslik, E. C., Laird, A. R., Fox, P. T., Radua, J., Mataix-Cols, D., … Eickhoff, S. B. (2018). Ten simple rules for neuroimaging meta-analysis. *Neuroscience and Biobehavioral Reviews, 84*, 151–161. https://doi.org/10.1016/j.neubiorev.2017.11.012 (November 2017).

Müller, V. I., Cieslik, E. C., Serbanescu, I., Laird, A. R., Fox, P. T., & Eickhoff, S. B. (2017). Altered brain activity in unipolar depression revisited: Meta-analyses of neuroimaging studies. *JAMA Psychiatry, 74*(1), 47–55. https://doi.org/10.1001/jamapsychiatry.2016.2783

Murdoch, B. E. (2010). The cerebellum and language: Historical perspective and review. *Cortex, 46*(7), 858–868. https://doi.org/10.1016/j.cortex.2009.07.018

Novick, J. M., Trueswell, J. C., & Thompson-Schill, S. L. (2005). Cognitive control and parsing: Reexamining the role of Broca's area in sentence comprehension. *Cognitive, Affective, & Behavioral Neuroscience, 5*(3), 263–281. https://doi.org/10.3758/CABN.5.3.263

Novick, J. M., Trueswell, J. C., & Thompson-Schill, S. L. (2010). Broca's area and language processing: Evidence for the cognitive control connection. *Language and Linguistics Compass, 4*(10), 906–924. https://doi.org/10.1111/j.1749-818X.2010.00244.x

Packard, M. G., & Knowlton, B. J. (2002). Learning and memory functions of the basal ganglia. *Annual Review of Neuroscience, 25*(1), 563–593. https://doi.org/10.1146/annurev.neuro.25.112701.142937

Pallier, C., Devauchelle, A.-D., & Dehaene, S. (2011). Cortical representation of the constituent structure of sentences. *Proceedings of the National Academy of Sciences, 108*(6), 2522–2527. https://doi.org/10.1073/pnas.1018711108

Papitto, G., Friederici, A. D., & Zaccarella, E. (2020). The topographical organization of motor processing: An ALE meta-analysis on six action domains and the relevance of Broca's region. *NeuroImage, 206*, Article 116321. https://doi.org/10.1016/j.neuroimage.2019.116321 (June 2019).

Parker, G. J. M., Luzzi, S., Alexander, D. C., Wheeler-Kingshott, C. A. M., Ciccarelli, O., & Lambon Ralph, M. A. (2005). Lateralization of ventral and dorsal auditory-language pathways in the human brain. *NeuroImage, 24*(3), 656–666. https://doi.org/10.1016/j.neuroimage.2004.08.047

Parola, A., Gabbatore, I., Bosco, F. M., Bara, B. G., Cossa, F. M., Gindri, P., & Sacco, K. (2016). Assessment of pragmatic impairment in right hemisphere damage. *Journal of Neurolinguistics, 39*. https://doi.org/10.1016/j.jneuroling.2015.12.003

Patel, S., Oishi, K., Wright, A., Sutherland-Foggio, H., Saxena, S., Sheppard, S. M., & Hillis, A. E. (2018). Right hemisphere regions critical for expression of emotion through prosody. *Frontiers in Neurology, 9*. https://doi.org/10.3389/fneur.2018.00224 (Apr).

Poeppel, D., Emmorey, K., Hickok, G., & Pylkkanen, L. (2012). Towards a new neurobiology of language. *Journal of Neuroscience, 32*(41), 14125–14131. https://doi.org/10.1523/JNEUROSCI.3244-12.2012

Powell, H. W. R., Parker, G. J. M., Alexander, D. C., Symms, M. R., Boulby, P. A., Wheeler-Kingshott, C. A. M., … Duncan, J. S. (2006). Hemispheric asymmetries in language-related pathways: A combined functional MRI and tractography study. *NeuroImage, 32*(1), 388–399. https://doi.org/10.1016/j.neuroimage.2006.03.011

Riedel, M. C., Ray, K. L., Dick, A. S., Sutherland, M. T., Hernandez, Z., Fox, P. M., … Laird, A. R. (2015). Meta-analytic connectivity and behavioral parcellation of the human cerebellum. *NeuroImage, 117*. https://doi.org/10.1016/j.neuroimage.2015.05.008

Robinson, J. L., Laird, A. R., Glahn, D. C., Blangero, J., Sanghera, M. K., Pessoa, L., … Fox, P. T. (2012). The functional connectivity of the human caudate: An application of meta-analytic connectivity modeling with behavioral filtering. *NeuroImage, 60*(1), 117–129. https://doi.org/10.1016/j.neuroimage.2011.12.010

Robinson, J. L., Laird, A. R., Glahn, D. C., Lovallo, W. R., & Fox, P. T. (2010). Metaanalytic connectivity modeling: Delineating the functional connectivity of the human amygdala. *Human Brain Mapping, 31*(2), 173–184. https://doi.org/10.1002/hbm.20854

Rodd, J. M., Vitello, S., Woollams, A. M., & Adank, P. (2015). Localising semantic and syntactic processing in spoken and written language comprehension: An Activation Likelihood Estimation meta-analysis. *Brain and Language, 141*, 89–102. https://doi.org/10.1016/j.bandl.2014.11.012

Rogalsky, C., & Hickok, G. (2009). Selective attention to semantic and syntactic features modulates sentence processing

networks in anterior temporal cortex. *Cerebral Cortex, 19*(4), 786–796. https://doi.org/10.1093/cercor/bhn126

Rorden, C., & Brett, M. (2000). Stereotaxic display of brain lesions. *Behavioural Neurology, 12*(4). https://doi.org/10.1155/2000/421719

Ross, E. D., & Mesulam, M. M. (1979). Dominant language functions of the right hemisphere?: Prosody and emotional gesturing. *Archives of Neurology, 36*(3). https://doi.org/10.1001/archneur.1979.00500390062006

Ross, E. D., & Monnot, M. (2008). Neurology of affective prosody and its functional-anatomic organization in right hemisphere. *Brain and Language, 104*(1). https://doi.org/10.1016/j.bandl.2007.04.007

Sahin, N. T., Pinker, S., & Halgren, E. (2006). Abstract grammatical processing of nouns and verbs in Broca's area: Evidence from fMRI. *Cortex, 42*(4), 540–562. https://doi.org/10.1016/S0010-9452(08)70394-0

Schell, M., Zaccarella, E., & Friederici, A. D. (2017). Differential cortical contribution of syntax and semantics: An fMRI study on two-word phrasal processing. *Cortex, 96*, 105–120. https://doi.org/10.1016/j.cortex.2017.09.002

Sebastian, A., Jung, P., Neuhoff, J., Wibral, M., Fox, P. T., Lieb, K., … Mobascher, A. (2016). Dissociable attentional and inhibitory networks of dorsal and ventral areas of the right inferior frontal cortex: A combined task-specific and coordinate-based meta-analytic fMRI study. *Brain Structure & Function, 221*(3), 1635–1651. https://doi.org/10.1007/s00429-015-0994-y

Segaert, K., Menenti, L., Weber, K., Petersson, K. M., & Hagoort, P. (2012). Shared syntax in language production and language comprehension-An fMRI study. *Cerebral Cortex, 22*(7), 1662–1670. https://doi.org/10.1093/cercor/bhr249

Stefaniak, J. D., Alyahya, R. S. W., & Lambon Ralph, M. A. (2021). Language networks in aphasia and health: A 1000 participant activation likelihood estimation meta-analysis. *NeuroImage, 233*, Article 117960. https://doi.org/10.1016/j.neuroimage.2021.117960 (February).

Stockbridge, M. D., Sheppard, S. M., Keator, L. M., Murray, L. L., Blake, M. L., Brownell, H., … Tompkins, C. (2021). Aprosodia subsequent to right hemisphere brain damage: A systematic review and meta-analysis. *Journal of the International Neuropsychological Society*, 1–27. https://doi.org/10.1017/S1355617721000825

Sundermann, B., & Pfleiderer, B. (2012). Functional connectivity profile of the human inferior frontal junction: Involvement in a cognitive control network. *BMC Neuroscience, 13*(1), 119. https://doi.org/10.1186/1471-2202-13-119

Tan, L. H., Chen, L., Yip, V., Chan, A. H. D., Yang, J., Gao, J. H., & Siok, W. T. (2011). Activity levels in the left hemisphere caudate-fusiform circuit predict how well a second language will be learned. *Proceedings of the National Academy of Sciences of the United States of America, 108*(6). https://doi.org/10.1073/pnas.0909623108

Thothathiri, M., Schwartz, M. F., & Thompson-Schill, S. L. (2010). Selection for position: The role of left ventrolateral prefrontal cortex in sequencing language. *Brain and Language, 113*(1), 28–38. https://doi.org/10.1016/j.bandl.2010.01.002

Tomasi, D., & Volkow, N. D. (2012). Resting functional connectivity of language networks: Characterization and reproducibility. *Molecular Psychiatry, 17*(8), 841–854. https://doi.org/10.1038/mp.2011.177

Torres, J., Drebing, D., & Hamilton, R. (2013). TMS and tDCS in post-stroke aphasia: Integrating novel treatment approaches with mechanisms of plasticity. *Restorative Neurology and Neuroscience, 31*(4), 501–515. https://doi.org/10.3233/RNN-130314

Tremblay, P., & Dick, A. S. (2016). Broca and Wernicke are dead, or moving past the classic model of language neurobiology. *Brain and Language, 162*, 60–71. https://doi.org/10.1016/j.bandl.2016.08.004

Turkeltaub, P. E., & Branch Coslett, H. (2010). Localization of sublexical speech perception components. *Brain and Language, 114*(1). https://doi.org/10.1016/j.bandl.2010.03.008

Turkeltaub, P. E., Coslett, H. B., Thomas, A. L., Faseyitan, O., Benson, J., Norise, C., & Hamilton, R. H. (2012). The right hemisphere is not unitary in its role in aphasia recovery. *Cortex, 48*(9), 1179–1186. https://doi.org/10.1016/j.cortex.2011.06.010

Turkeltaub, P. E., Eickhoff, S. B., Laird, A. R., Fox, M., Wiener, M., & Fox, P. (2012). Minimizing within-experiment and within-group effects in activation likelihood estimation meta-analyses. *Human Brain Mapping, 33*(1), 1–13. https://doi.org/10.1002/hbm.21186

Ullman, M. T. (2001). A neurocognitive perspective on language: The declarative/procedural model. *Nature Reviews Neuroscience, 2*(10), 717–726. https://doi.org/10.1038/35094573

Ullman, M. T. (2004). Contributions of memory circuits to language: The declarative/procedural model. *Cognition, 92*(1–2), 231–270. https://doi.org/10.1016/j.cognition.2003.10.008

Ullman, M. T. (2016). The declarative/procedural model: A neurobiological model of language learning, knowledge, and use. In *Neurobiology of language* (pp. 953–968). Elsevier. https://doi.org/10.1016/B978-0-12-407794-2.00076-6.

Vigneau, M., Beaucousin, V., Hervé, P. Y., Duffau, H., Crivello, F., Houdé, O., … Tzourio-Mazoyer, N. (2006). Meta-analyzing left hemisphere language areas: Phonology, semantics, and sentence processing. *NeuroImage, 30*(4), 1414–1432. https://doi.org/10.1016/j.neuroimage.2005.11.002

Vigneau, M., Beaucousin, V., Hervé, P.-Y., Jobard, G., Petit, L., Crivello, F., … Tzourio-Mazoyer, N. (2011). What is right-hemisphere contribution to phonological, lexico-semantic, and sentence processing? *NeuroImage, 54*(1), 577–593. https://doi.org/10.1016/j.neuroimage.2010.07.036

Viñas-Guasch, N., & Wu, Y. J. (2017). The role of the putamen in language: A meta-analytic connectivity modeling study. *Brain Structure & Function, 222*(9), 3991–4004. https://doi.org/10.1007/s00429-017-1450-y

Walenski, M., Europa, E., Caplan, D., & Thompson, C. K. (2019). Neural networks for sentence comprehension and production: An ALE-based meta-analysis of neuroimaging studies. *Human Brain Mapping, 40*(8), 2275–2304. https://doi.org/10.1002/hbm.24523

Wang, J., Fan, L., Wang, Y., Xu, W., Jiang, T., Fox, P. T., … Jiang, T. (2015). Determination of the posterior boundary of Wernicke's area based on multimodal connectivity profiles. *Human Brain Mapping, 36*(5), 1908–1924. https://doi.org/10.1002/hbm.22745

Wang, J., Yang, Y., Fan, L., Xu, J., Li, C., Liu, Y., … Jiang, T. (2015). Convergent functional architecture of the superior parietal lobule unraveled with multimodal neuroimaging approaches. *Human Brain Mapping, 36*(1). https://doi.org/10.1002/hbm.22626

Wheatley, T., Weisberg, J., Beauchamp, M. S., & Martin, A. (2005). Automatic priming of semantically related words reduces activity in the fusiform gyrus. *Journal of Cognitive Neuroscience, 17*(12). https://doi.org/10.1162/089892905775008689

Wildgruber, D., Ackermann, H., & Grodd, W. (2001). Differential contributions of motor cortex, basal ganglia, and cerebellum to speech motor control: Effects of syllable repetition rate evaluated by fMRI. *NeuroImage, 13*(1). https://doi.org/10.1006/nimg.2000.0672

Wojtasik, M., Bludau, S., Eickhoff, S. B., Mohlberg, H., Gerboga, F., Caspers, S., & Amunts, K. (2020). Cytoarchitectonic characterization and functional decoding of four new areas in the human lateral orbitofrontal cortex. *Frontiers in Neuroanatomy, 14*, 1–18. https://doi.org/10.3389/fnana.2020.00002 (February).

Xiang, H.-D., Fonteijn, H. M., Norris, D. G., & Hagoort, P. (2010). Topographical functional connectivity pattern in the perisylvian language networks. *Cerebral Cortex, 20*(3), 549–560. https://doi.org/10.1093/cercor/bhp119

Xu, J., Kemeny, S., Park, G., Frattali, C., & Braun, A. (2005). Language in context: Emergent features of word, sentence, and narrative comprehension. *NeuroImage, 25*(3), 1002–1015. https://doi.org/10.1016/j.neuroimage.2004.12.013

Zaccarella, E., Schell, M., & Friederici, A. D. (2017). Reviewing the functional basis of the syntactic merge mechanism for language: A coordinate-based activation likelihood estimation meta-analysis. *Neuroscience and Biobehavioral Reviews, 80*, 646–656. https://doi.org/10.1016/j.neubiorev.2017.06.011 (July).

Zempleni, M., Renken, R., Hoeks, J. C. J., Hoogduin, J. M., Stowe, L. A., Willems, R. M., … Herrmann, M. (1998). Cerebral pathways in processing of affective prosody: A dynamic causal modeling study. *NeuroImage, 12*(2), 188–197.

Zhang, Q., Wang, H., Luo, C., Zhang, J., Jin, Z., & Li, L. (2019). The neural basis of semantic cognition in Mandarin Chinese: A combined fMRI and TMS study. *Human Brain Mapping, 40*(18), 5412–5423. https://doi.org/10.1002/hbm.24781

Zhu, Z., Bastiaansen, M., Hakun, J. G., Petersson, K. M., Wang, S., & Hagoort, P. (2019). Semantic unification modulates N400 and BOLD signal change in the brain: A simultaneous EEG-fMRI study. *Journal of Neurolinguistics, 52*, Article 100855. https://doi.org/10.1016/j.jneuroling.2019.100855 (July).

Zou, L., Ding, G., Abutalebi, J., Shu, H., & Peng, D. (2012). Structural plasticity of the left caudate in bimodal bilinguals. *Cortex, 48*(9). https://doi.org/10.1016/j.cortex.2011.05.022